Death-Associated Protein Kinase 1 Dampens Keratinocyte Necroptosis and Expression of Inflammatory Genes in Lichen Planus

JID Open

Nils Kurzen[1,7], Menna Mubarak[1,2,7], Jessica Eigemann[1,3], Peter Seiringer[1], Sophia Wasserer[1], Christina Hillig[4], Michael Menden[4,5], Tilo Biedermann[1], Carsten B. Schmidt-Weber[3], Kilian Eyerich[2], Manja Jargosch[1,3], Stefanie Eyerich[3] and Felix Lauffer[1,6]

Journal of Investigative Dermatology (2025) **145,** 1921−1929; doi:10.1016/j.jid.2024.11.017

Lichen planus (LP) is a chronic inflammatory disease affecting the skin, mucosa, nail, and hair. Previous studies demonstrated a pivotal role of type 1 immunity in LP because infiltrating T cells trigger apoptosis and necroptosis in the epidermis. In this study, we investigated the role of DAPK1 in LP with special focus on its role in mediating cell death and inflammation. Bulk RNA sequencing of skin biopsies revealed a high expression of *DAPK1* in LP compared with that in psoriasis and atopic dermatitis. DAPK1 expression in human keratinocytes was induced by IFN-γ, TNF, and IL-32. CRISPR/Cas9-mediated *DAPK1* knockout led to a decreased rate of cell death and induction of proapoptotic proteins (BAX, cPARP) in human keratinocytes upon stimulation with the supernatant T cells derived from LP skin biopsies. Meanwhile, *DAPK1* knockout resulted in an induction of kinases involved in necroptosis (RIPK3) and an upregulation of inflammatory genes (*CXCL9*, *CXCL10*, *CXCL11*, *IL32*, *CCL2*) after stimulation with LP supernatant T cells. In summary, we demonstrate that DAPK1 mediates keratinocyte apoptosis under type 1 inflammatory conditions and thereby counteracts necroptosis and regulation of inflammatory genes. These findings point toward previously unreported therapeutic approaches for activating or stabilizing DAPK1 in LP.

Keywords: Apoptosis, Death-associated protein kinase 1, Interface dermatitis, Lichen planus, Necroptosis

INTRODUCTION

Lichen planus (LP) is one of the most common noncommunicable inflammatory skin diseases (ISDs) with an estimated prevalence of 0.1−1% (Schruf et al, 2022). LP presents either as polygonal papules at the flexures of the extremities or as exanthematic variant affecting the whole body. Furthermore, LP can occur at oral and genital mucosa and may lead to scarring alopecia when involving hair follicles. Patients suffer from severe itch, low QOL, and social stigmatization (Boehncke and Schön, 2015; Brunner et al, 2017; Eyerich and Eyerich, 2018; Fiocco et al, 2021). LP is still a difficult-to-treat skin disease because no targeted therapy has been approved so far.

In skin histology, LP is characterized by a saw-shaped acanthosis with orthohyperkeratosis and focal hypergranulosis as well as a lichenoid interface dermatitis (ID) (Lauffer et al, 2018). The latter is defined as a subepidermal band-like lymphocytic infiltrate accompanied by cell death of single keratinocytes in the basal compartment of the epidermis (Sontheimer, 2009). Our group and others demonstrated that ID is caused by a type 1 dominant immune response, in which IFN-γ and TNF mediate apoptosis and necroptosis of keratinocytes (Lauffer et al, 2018; Wenzel and Tüting, 2008). Whereas apoptosis does not trigger an inflammatory immune response, necroptosis is highly immunogenic because it leads to a disruption of the cell membrane and a release of danger-associated molecular patterns (Khoury et al, 2020). Factors directing keratinocytes to undergo either of these cell death mechanisms in LP remain poorly understood (Lauffer et al, 2018).

Using large transcriptome datasets of human skin biopsies of ISDs, we associated with disease characteristics such as ID. One of these is DAPK1, which has previously not been investigated in type 1 ISDs. DAPK1 is involved in various pro and anti-inflammatory processes (Lai and Chen, 2014), such viral infections and antitumor immunity (Barathan et al, 2015; Lee et al, 2011; Wang et al, 2020b; Wei et al, 2021).

[1]Department of Dermatology and Allergy, Technical University of Munich, Munich, Germany; [2]Department of Dermatology and Venereology, Medical Center, University of Freiburg, Freiburg, Germany; [3]Center of Allergy and Environment (ZAUM), Technical University and Helmholtz Center Munich, Munich, Germany; [4]Computational Health Center, Institute of Computational Biology, Helmholtz Munich, Neuherberg, Germany; [5]Department of Biochemistry & Pharmacology, Bio21 Molecular Science and Biotechnology Institute, The University of Melbourne, Australia; and [6]Department of Dermatology and Allergy, Ludwig-Maximilians University Hospital, Munich, Germany

[7]These authors contributed equally to this work.

Correspondence: Felix Lauffer, Department of Dermatology and Allergy, Ludwig-Maximilians University Hospital, Frauenlobstraße 9 − 11, Munich 80337, Germany. E-mail: Felix.Lauffer@med.uni-muenchen.de

Abbreviations: AD, atopic dermatitis; ID, interface dermatitis; ISD, inflammatory skin disease; KO, knockout; LP, lichen planus; LP-TCS, lichen planus−derived T cell supernatant; RNP, ribonucleoprotein

Received 27 February 2024; revised 30 October 2024; accepted 12 November 2024; accepted manuscript published online 31 December 2024; corrected proof published online 31 January 2025

Besides, it has been described as a tumor suppressor in various cancers (Singh et al, 2016) because it has proapoptotic functions in human ovarian carcinoma cell lines (Yoo et al, 2012). DAPK1 is induced by IFN-γ in human ovarian carcinoma cell lines and inhibits NF-kB activation (Yoo et al, 2012). Furthermore, IL-32 mediates DAPK1 phosphorylation in macrophage such as THP-1 cells (Turner-Brannen et al, 2011). DAPK1 has various autophosporylation sites, which function as positive (Ser734) or negative (Ser308) regulators (Kim et al, 2019).

In this study, we sought to investigate the role of the DAPK1 in LP, with special attention to regulated cell death and inflammation in keratinocytes. We demonstrate an upregulation of DAPK1 at the dermoepidermal junction of LP by spatial transcriptomics and immunohistochemistry. In human keratinocytes, IFN-γ, TNF, and IL-32 trigger DAPK1 induction. Furthermore, we examined the effects of *DAPK1* knockout (KO) in primary human keratinocytes and reconstructed human epidermis models. In this study, we found proapoptotic and anti-inflammatory effects of DAPK1, highlighting DAPK1 as a hub kinase favoring apoptosis and preventing necroptosis as well as expression of inflammatory genes.

RESULTS

DAPK1 is enriched in basal human keratinocytes in LP and correlates with the strength of ID

In previous work of our group, Batra et al (2021[1]) created a network of genes associated with different clinical and histological hallmarks of various ISDs, such as acanthosis, the presence of neutrophils, or skin dryness. Within these, we found *DAPK1* to be associated with ID (Figure 1a). To validate the strength of the association, we performed a correlation analysis of *DAPK1* gene expression and the strength of ID rated from 0 to 3 by 2 independent dermatopathologists (Figure 1b). In this study, we found a positive correlation between *DAPK1* expression and the strength of ID ($P < .0001$, $r = 0.4808$), indicating a pivotal role in ID. Using bulk RNA sequencing of LP (n = 30), AD (n = 48), psoriasis (n = 90), and nonlesional skin biopsies (n = 168) (Batra et al, 2021[1]) (patient's characteristics are listed in Supplementary Table 1), we found that *DAPK1* gene expression was significantly upregulated in LP lesions compared with that in nonlesional skin ($P = .0001$) as well as with that in AD and psoriasis ($P < .0001$) (Figure 1c). In addition, spatial transcriptomics revealed highest numbers of *DAPK1* transcripts in the basal epidermis and the dermoepidermal junction (dermis depth 1) of LP (unique molecular identifier counts ≥ 1−100) in contrast to that in nonlesional skin (unique molecular identifier counts ≥ 1−50), psoriasis (unique molecular identifier count ≥ 1−10), and AD (unique molecular identifier count ≥ 1−10) (Figure 1d and e). In LP, the number of *DAPK1* transcripts gradually decreased from basal to upper epidermis and from dermis depth 1 to 5. To further characterize DAPK1 on protein level, we performed immunohistochemical staining in LP (n = 4), nonlesional LP (n = 3), and psoriasis (n = 3) skin biopsies. DAPK1 was enriched in the basal keratinocytes of LP in contrast to that in nonlesional ($P = .0080$) or psoriasis ($P = .0092$) skin (Figure 1f and g).

DAPK1 is induced by type 1 cytokines in human keratinocytes

Next, we aimed to identify upstream inducers of DAPK1. We therefore stimulated keratinocytes with different cytokines and cytokine combinations. IFN-γ and TNF stimulation resulted in the strongest DAPK1 induction than type 2 (IL-4 + IL-13) and type 3 (IL-17A, TNF) cytokines (Figure 2a). This effect was enhanced by an additional stimulation with IL-32 ($P < .05$), another known inducer of DAPK1 (Turner-Brannen et al, 2011), whereas IL-32 alone was insufficient to induce DAPK1 in keratinocytes (Figure 2b–d). Interestingly, we could find an induction of the activating 734 serin phosphorylation chain after stimulation with IFN-γ + TNF ($P < .05$) as well as IFN-γ + TNF + IL-32 ($P < .005$) (Figure 2e and f).

Using bulk RNA-sequencing data (Batra et al, 2021[1]) of lesional and nonlesional biopsies (287 patients) covering 13 different diagnoses of ISDs, we correlated *DAPK1* gene expression to various type 1−, type 2−, and type 17−related genes. In this study, we could observe the strongest positive correlation of *DAPK1* to type 1 genes such as *CXCL9* ($P < .0001$, $r = 0.363$), *CXCL10* ($P < .0001$, $r = 0.361$), signal transducer and activator of transcription 2 gene *STAT2* ($P < .0001$, $r = 0.387$), and signal transducer and activator of transcription 4 gene *STAT4* ($P < .0001$, $r = 0.393$). In line with that, type 3 genes such as *IL17A* ($P < .0001$, $r = -0.358$) and *IL17F* ($P < .0001$, $r = -0.3071$) were negatively correlated to *DAPK1*. We also observed a significant positive correlation to *IFNG* gene expression ($P < .0001$, $r = 0.257$) (Figure 2g and h).

DAPK1 KO leads to decreased cell death in reconstructed human epidermis models under type 1 inflammatory conditions

Next, we investigated the function of DAPK1 in keratinocytes under type 1 inflammatory conditions. First, we examined DAPK1 in a protein−protein interaction network using STRING-Cytoscape. DAPK1 showed connections to autophagic proteins (ATG3/5/12/14), inflammatory proteins (MAPK1/3), and proteins of the CALM family, which are known to regulate NF-κB. Besides, there were various connections to apoptotic proteins CASP3 and CASP8 as well as to RIPK3, which is involved in necroptosis (Figure 3a). The pathway analysis further revealed an enrichment of the NOD-like receptor pathway; TNF signaling; and the pathways of cell death, survival, and viral infections. The full list of enriched pathways can be found in the Supplementary Table S2.

Next, we performed *DAPK1* KO in primary human keratinocytes using CRISPR/Cas9. After confirming the KO efficiency of *DAPK1* ($P < .0001$) (Supplementary Figure S1a and b), we stimulated primary keratinocytes with the supernatant of T cells derived from LP skin biopsies (ie, LP-derived T cell supernatant [LP-TCSs]). IFN-γ (96780 pg/ml), TNF (55570 pg/ml), and IL-32 (616 pg/ml) were among the cytokines with the highest concentrations in LUMINEX analysis (Supplementary Figure S1c). We then performed a cell viability assay of *DAPK1*-KO cells stimulated with the LP-TCS. In this study,

[1] Batra R, Garzorz-Stark N, Lauffer F, Jargosch M, Pilz C, Roenneberg S, et al. Integration of phenomics and transcriptomics data to reveal drivers of inflammatory processes in the skin. bioRxiv 2021.

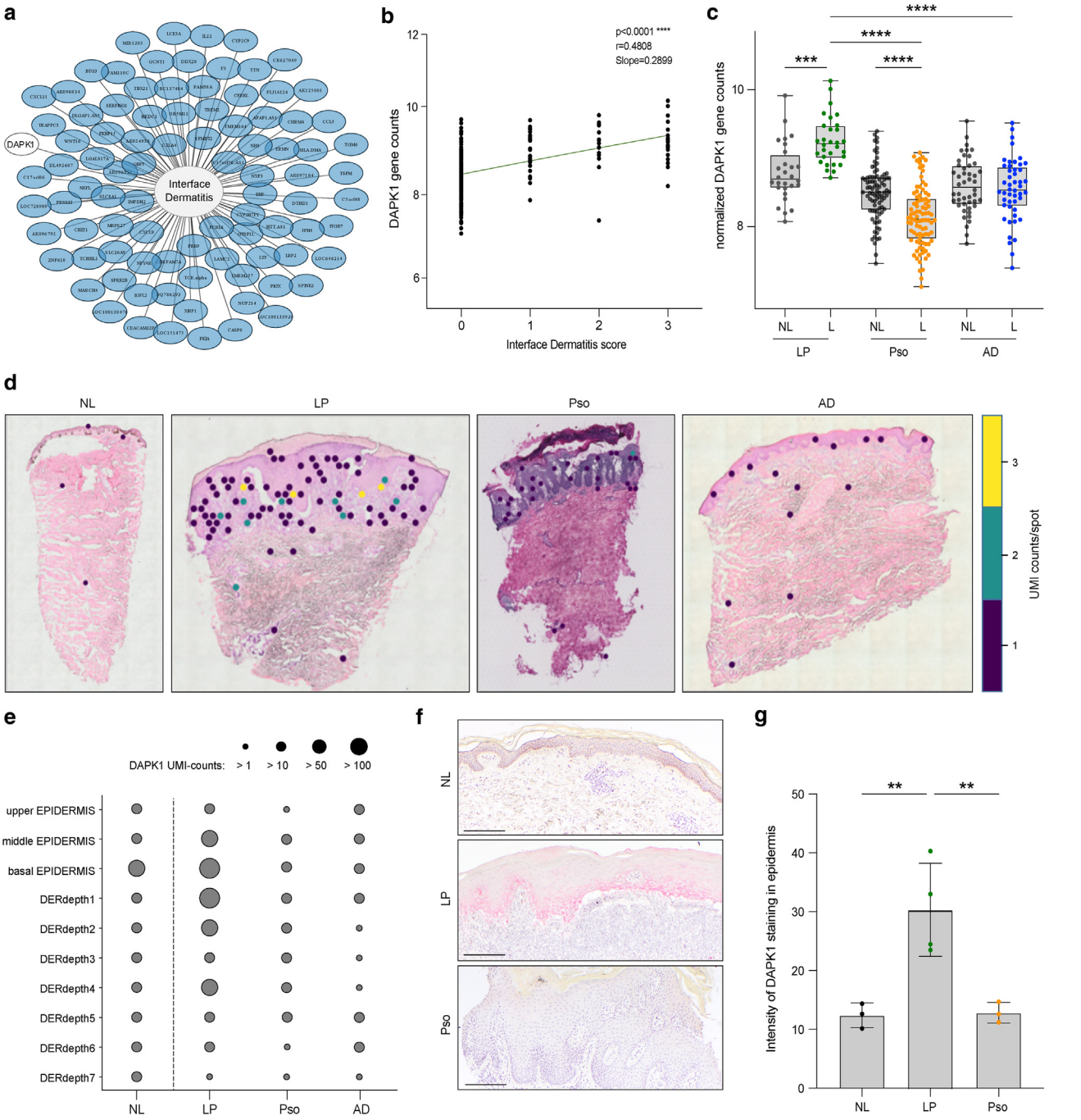

Figure 1. DAPK1 is enriched in basal human keratinocytes in LP and correlates with the strength of ID. (**a**) ID gene cluster network from Batra et al, 2021.[1] (**b**) Correlation analysis of *DAPK1* gene expression from bulk RNA sequencing and the strength of ID in ISD (n = 287) with 0 (no ID), 1 (mild ID), 2 (moderate ID), and 3 (severe ID). Linear regression calculation was performed with Pearson correlation. (**c**) Normalized gene counts of *DAPK1* in lesional skin (L) of patients with LP (n = 30), Pso (n = 90), and AD (n = 48) compared with that in autologous nonlesional skin (n = 168) analyzed by bulk RNA sequencing. Each dot represents 1 patient biopsy. (**d**, **e**) Spatial transcriptomic expression of *DAPK1* transcripts in nonlesional (NL, n = 14) and lesional LP (n = 11), AD (n = 9), and Pso (n = 11) skin biopsies. Shown are representative data (UMI counts/spot) from 1 biopsy per condition (for **d**) and quantified data for all biopsies separated by epidermis and dermis depths (total UMI counts) (for **e**). (**f, g**) Immunohistochemical staining of DAPK1 in NL (n = 3), LP (n = 4), and psoriasis (n = 3) skin biopsies. Representative pictures are shown in **f**, and the bar represents 100 μm. (**g**) Epidermal DAPK1 protein expression was quantified using color deconvolution in ImageJ. Significance between disease groups was tested by ordinary 1-way ANOVA test with Tukey's multiple comparison. ****$P < .0001$ and **$P < .01$. L denotes lesional, NL denotes nonlesional, and Pso denotes psoriasis. AD, atopic dermatitis; ID, interface dermatitis; LP, lichen planus; IHC, immunohistochemistry; ISD, inflammatory skin disease; UMI, unique molecular identifier.

DAPK1 KO led to an increased cell viability compared with wild-type keratinocytes (denoted as noRNP) (Figure 3b). In reconstructed human epidermis models, LP-TCS induced cell death, which was reflected in histological changes such as swelling and vacuolization of the keratinocytes. Moreover, *DAPK1* KO led to a reduction in the number of dead cells

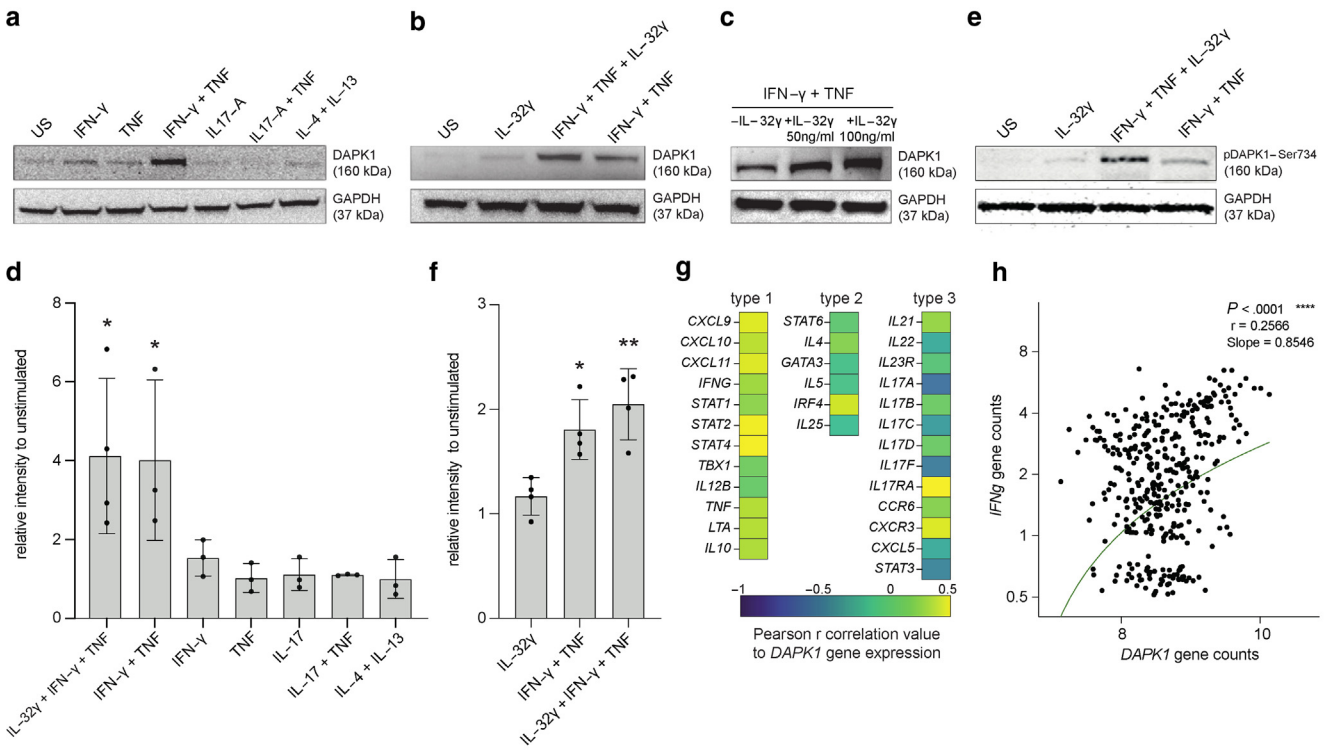

Figure 2. DAPK1 is induced by type 1 cytokines in human keratinocytes. (**a**–**d**) DAPK1 induction in primary human keratinocytes under different inflammatory cytokine conditions as indicated. Keratinocytes were stimulated for 48 h and subsequently analyzed by western blot. The following stimulations were used for (**a**) IFN-γ, TNF, IFN-γ + TNF, IL-17A, IL-17A + TNF, IL-4 + IL-13, IL-1β, and IFN-α (each 50 ng/ml); for (**b**) IL-32, IFN-γ + TNF + IL-32, and IFN-γ + TNF (each 50 ng/ml); and for (**c**) IFN-γ + TNF (each 50 ng/ml) and IFN-γ + TNF (each 50 ng/ml) + IL-32 (50 or 100 ng/ml). **(d)** Quantification of DAPK1 protein expression in keratinocytes (n = 3–4) of western blot from **a**–**c** relative to unstimulated control after stimulation with inflammatory cytokines. (**e, f**) Western blot analysis of DAPK1 phosphorylation (pDAPK1-Ser734) upon stimulation with the indicated cytokines IL-32, IFN-γ + TNF + IL-32, and IFN-γ + TNF (each 50 ng/ml), with **e** showing a representative western blot and **f** showing the quantification of pDAPK1 signal intensity (n = 4). (**g**) Heat map of correlation analysis of *DAPK1* gene expression to type 1, type 2, and type 3 genes in a bulk RNA dataset of 13 different inflammatory skin diseases (Batra et al, 2021). The significance of linear regression was calculated with Pearson correlation. (**h**) Correlation of *DAPK1* and *IFNG* gene expressions in lesional skin of patients with inflammatory skin diseases (n = 287) analyzed by bulk RNA sequencing. Each dot represents 1 patient. Significance of linear regression was calculated with Pearson correlation. Significance between stimulation conditions was tested by paired *t*-test. *$P < .05$. h, hour.

($P < .001$) and the epidermal thickness ($P < .005$) after stimulation with the LP-TCS (Figure 3c–e).

DAPK1 induces apoptosis and dampens the expression of inflammatory genes under type 1 conditions

Next, we focused on different forms of regulated cell death. *DAPK1* KO resulted in an upregulation of genes involved in necroptosis (*RIPK3* [$P < .005$], *MLKL* [$P < .05$]) compared with noRNP cells, whereas genes involved in apoptosis (*BAX* and *BCL2)* were not affected (Figure 4a). However, after stimulation with LP-TCS, PARP ($P < .005$) and BAX ($P < .05$) proteins were significantly downregulated, while RIPK3 was upregulated ($P < .05$) in *DAPK1*-KO cells, indicating that DAPK1 promotes apoptosis and prevents necroptosis (Figure 4b and c). Consistent with this observation, keratinocytes showed a significant enhancement of DAPK1 protein expression ($P < .05$) upon stimulation with IFN-γ and TNF under necroptotic conditions by treatment with Z-VAD, a panapoptosis blocker (Supplementary Figure S2a and b). Furthermore, *DAPK1* KO resulted in a higher release of IL-1β (1.87 ± 0.19, $P = .0029$) and IL-18 (1.21 ± 0.16, $P = .0367$) than noRNP control (Figure 4d and e and Supplementary Figure S2c and d). In line with these observations, *DAPK1* KO led to an enhanced expression of chemokines and cytokines, which are typically upregulated in LP (Dickman et al, 2022; Wenzel et al, 2008) (*CXCL9* [$P < .005$], *CXCL10* [$P < .05$], *CXCL11* [$P < .05$], *CCL2* [$P < .05$], *IL1β* [$P < .005$], *IL32* [$P < .05$]), compared with the noRNP cells (Figure 4f). In conclusion, DAPK1 promotes apoptosis and inhibits the release of IL-1β and IL-18 as well as the expression of inflammatory genes within the inflammatory milieu of LP.

DISCUSSION

In this study, we demonstrate that DAPK1 is specifically upregulated in the dermoepidermal junction of LP. Although it is well-known that type 1 immunity induces inflammatory cell death in LP (Freund et al, 2023; Kim et al, 2015; Lauffer et al, 2018), we discovered that an activation of DAPK1 by type 1 cytokines mediates apoptosis and reduces the expression of inflammatory cytokines. This might counteract

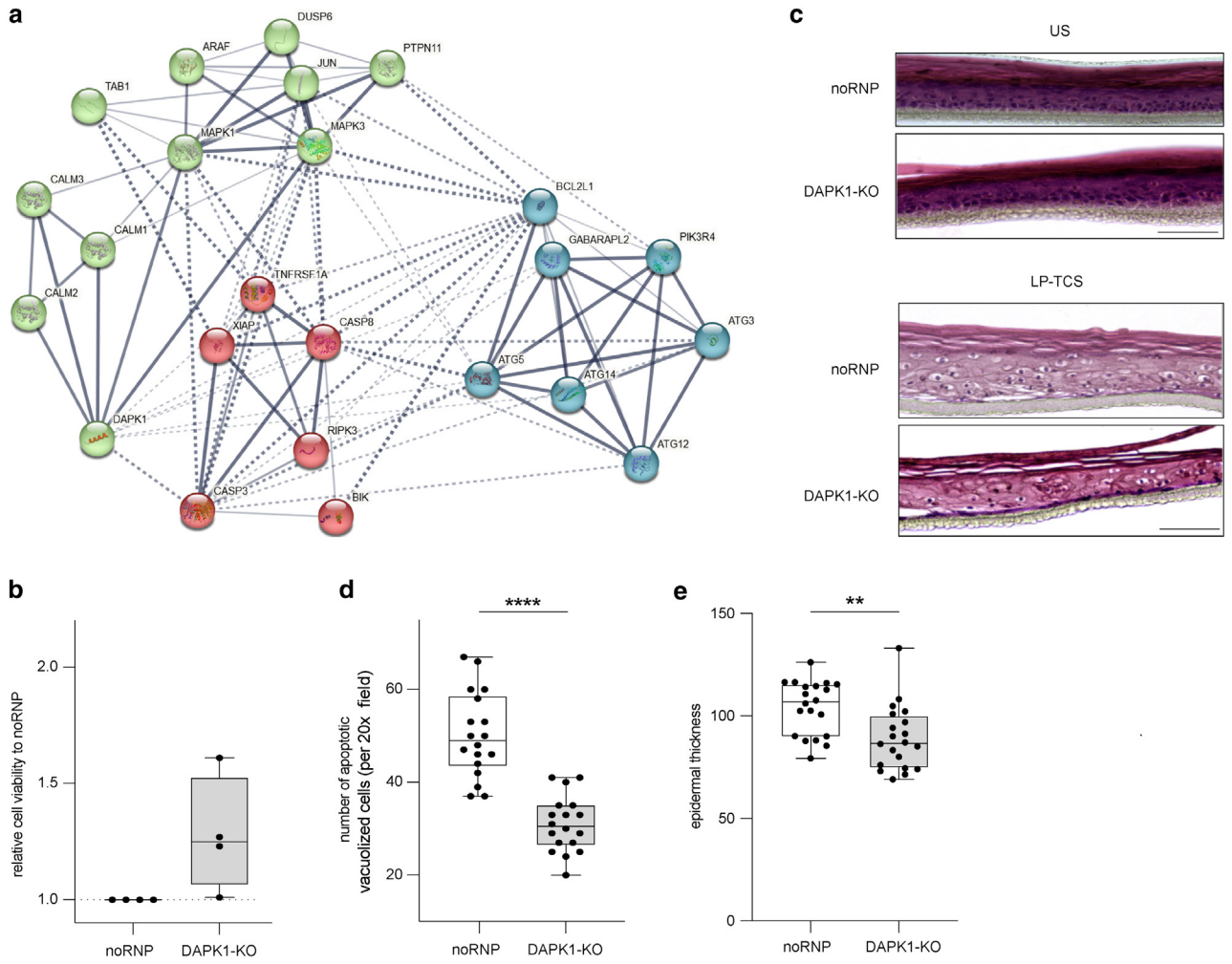

Figure 3. *DAPK1* KO leads to decreased cell death in RHE models under type 1 inflammatory conditions. (**a**) DAPK1 STRING protein–protein interaction network using Cytoscape for visualization. Each color represents a functional gene cluster group, with red denoting apoptosis, blue denoting autophagy, and green denoting regulatory proteins of different cell death and inflammatory pathways. Network nodes represent proteins, and edges represent protein–protein interactions, with the line thickness visualizing interaction confidence. Dotted lines display interactions between the different clusters. **(b)** Relative cell viability of *DAPK1*-KO keratinocytes (n = 4) compared with that of wild-type cells (noRNP) upon 24-h stimulation with lesional LP-TCS. **(c–e)** H&E staining of wild-type (noRNP) and *DAPK1*-KO RHE models (n = 3), which were stimulated with lesional LP-TCS for 72 h compared with the unstimulated (denoted as US). Representative H&E staining is shown in **c**, and bar indicates 100 μm. The number of visible dead cells and epidermal thickness was quantified under LP-TCS conditions for noRNP and *DAPK1* KO in **d** and **e** (n = 18). Paired *t*-test was used for significance analysis between noRNP and *DAPK1* KO. $^{**}P < .01$ and $^{****}P < .0001$. US denotes unstimulated. h, hour; KO, knockout; LP, lichen planus; LP-TCS, lichen planus–derived T cell supernatant; RHE, reconstructed human epidermis.

inflammatory cell death and thereby contribute to the chronification of skin inflammation.

Although therapeutic options for the 2 most common ISD—psoriasis and AD—are continuously increasing, there is still a lack of targeted therapies for type 1 ISD. This group comprises several ISDs that share the pathogenic event of cytotoxic immune reactions against keratinocytes, hair follicles, or melanocytes. Typical examples are LP, cutaneous lupus erythematosus, dermatomyositis, vitiligo, and alopecia areata (Eyerich and Eyerich, 2018). IFN-γ and TNF are the main drivers of keratinocyte apoptosis and necroptosis in ID (Lauffer et al, 2018; Shao et al, 2019).

In our study, we assessed the effects of DAPK1 in the type 1 cytokine milieu of LP. Indeed, we observed an induction of DAPK1 by IFN-γ and TNF, which was potentiated by IL-32. DAPK1 was previously described as a tumor suppressor in various cancers: loss of DAPK1 is associated with a poorer prognosis in colon and bladder cancer, and *DAPK1* KO leads to more invasiveness and metastasis in animal models of colorectal cancer (Steinmann et al, 2019; Xie et al, 2017). Interestingly, *DAPK1* KO aggravated oxidative stress, cell death, and inflammation in lipopolysaccharide-induced acute lung injury model, pointing toward a protective role in inflammatory diseases (Li et al, 2020). In line with these observations, a role of DAPK1 in ventilator-induced lung injury was described and appears to trigger alveolar epithelial cell apoptosis (Wang et al, 2022, 2020a). These results are in concordance with our results demonstrating that *DAPK1* KO diminished apoptosis and led to increased inflammation of keratinocytes.

Identifying the factors orchestrating the balance between apoptosis and necroptosis might lead to identification of

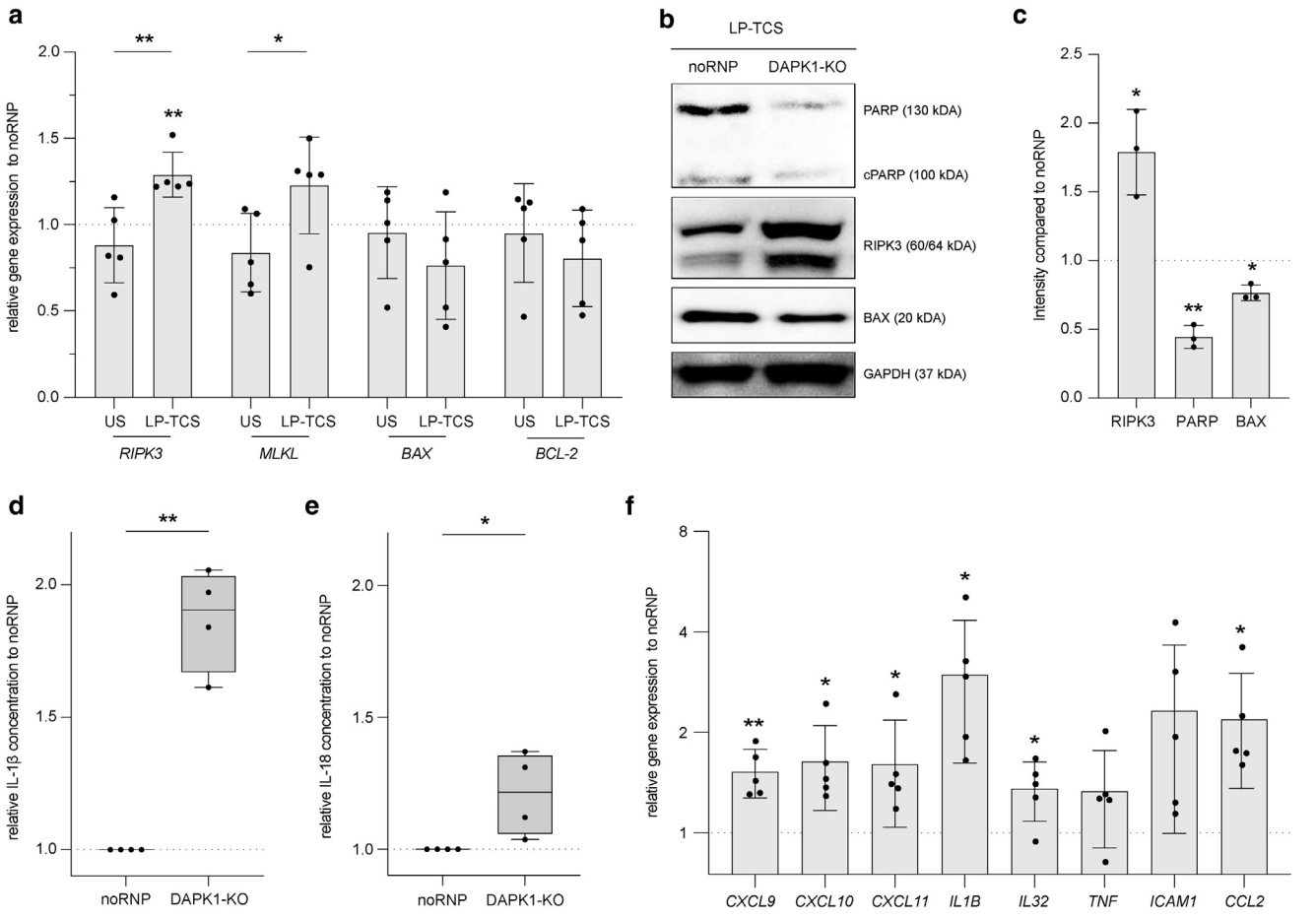

Figure 4. DAPK1 induces apoptosis and dampens the expression of inflammatory genes under type 1 conditions. (**a**) Relative expression of genes involved in necroptosis (*RIPK3*, *MLKL*) and apoptosis (*BAX*, *BCL-2*) analyzed by qPCR in DAPK1-KO compared with that in noRNP keratinocytes (n = 5) left unstimulated and after stimulation with an LP-TCS. **(b, c)** Western blot analysis of apoptotic (PARP, cPARP, BAX) and necroptotic (RIPK3, pRIPK3) proteins in wild-type (noRNP) and *DAPK1*-KO keratinocytes upon 48-h stimulation with LP-TCS. Representative western blot results are shown in **b**, and quantification (n = 3) of protein expression relative to unstimulated control is shown in **c**. (**d, e**) Protein concentration of the secreted inflammatory cytokines (**d**) IL-1β and (**e**) IL-18 in supernatants of wild-type (noRNP) and *DAPK1*-KO keratinocytes (n = 4) upon stimulation with lesional LP-TCS for 24 h measured by ELISA. (**f**) qPCR analysis of relative gene expression of chemokines (*CXCL9*, *CXCL10*, *CXCL11*, *CCL2*), proinflammatory cytokines (*IL1β*, *IL32*, *TNF*), and adhesion molecule (*ICAM1*) in *DAPK1*-KO keratinocytes compared with that in noRNP keratinocytes (n = 5) after stimulation with an LP-TCS. Paired *t*-test was used for significance analysis between noRNP and *DAPK1* KO. $*P < .05$ and $**P < .01$. US denotes unstimulated. h, hour; KO, knockout; LP-TCS, lichen planus–derived T cell supernatant.

previously unreported therapeutic approaches for LP. Several compounds inhibiting inflammatory cell death have been developed, although none has reached approval for clinical use so far (Chen et al, 2022). Our results point toward another drug-targeting approach: stabilizing the antinecroptotic, proapoptotic function of DAPK1 in LP. In fact, drug strategies to activate DAPK1 are currently in development for cancer treatment. Panobinostat (LBH589), a pan-histone deacetylase, activates DAPK1 kinase activity by inhibiting the inactivating Ser308 autophosphorylation of the DAPK1 protein. This leads to increased autophagy and apoptosis in colon cancer cell lines (Chen et al, 2019; Gandesiri et al, 2012). However, Panobinostat does not specifically interact with DAPK1, which is why drugs solely targeting the Ser308 or the Ser734 phosphorylation site are desirable. Future studies are necessary to investigate the clinical benefit of specific DAPK1 modulation for the treatment of LP.

In summary, we demonstrated that DAPK1 is highly expressed in LP and prevents keratinocyte necroptosis. Given the high need of further therapeutic options for type 1 dominant inflammatory diseases, our data point toward a previously unreported therapeutic approach of stabilizing DAPK1 function to counteract inflammatory cell death and perpetuation of skin inflammation in LP.

MATERIALS AND METHODS

Patient cohort

All materials of patients in this study were used after receiving written informed consent to be part of the Biobank Biederstein. The study was approved by the local ethics committee of the Technical University Munich (ethical vote), and all experiments were performed in accordance with the Declaration of Helsinki.

CRISPR/Cas9

CRISPR/Cas9 KO of *DAPK1* was performed by application of ribonucleoprotein (RNP) complexes with the 4D-Nucleofector device (Lonza) using the P3 Primary Cell 4D-Nucleofector X Kit S (Lonza).

Formation of RNP complexes. Predesigned target CRISPR RNA Hs.Cas9.DAPK1.1.AA (Integrated DNA Technologies) and tracrRNA (Integrated DNA Technologies) were mixed with IDTE buffer for a

final concentration of 200 μM. DAPK1 CRISPR RNA was hybridized to tracrRNA (Integrated DNA Technologies, number 1072534) in equimolar ratios by 5-minute incubation at 95 °C after a slow cool down to room temperature. Then, RNP formation was performed by mixing 180 pmol CRISPR RNA-tracrRNA duplex with 60 pmol Cas9 protein in nucleofection buffer P3 and incubating for 20 minutes at room temperature.

Transfection of RNP complexes. A total of 1.6×10^5 primary keratinocytes were diluted in 16 μl P3 buffer and mixed with 4 μl of either the preformed RNP complex for DAPK1 (*DAPK1* KO) or with P3 buffer instead of RNP complexes as a control (noRNP). The 0.15E06 cells of the *DAPK1* KO mix were transferred in a small cuvette, and 0.6E06 cells of the noRNP mix were transferred in a big cuvette and electroporated with the pulse DS-138 in the 4D Nucleofector unit. After 10 minutes resting phase at room temperature, they were cultured in DermaLife Basal Medium with supplements for further experiments. KO efficiency was confirmed by western blot analysis.

Spatial transcriptomics

Spatial transcriptomics data were derived from previous work of our group. Patient characteristics and data analysis are described previously (Schäbitz et al, 2022). In total, 31 patients were included in the analysis (nonlesional = 14, LP = 11, AD = 9, and psoriasis = 11).

Bulk RNA sequencing

Bulk RNA sequencing data were derived from previous work of our group. Patient characteristics and data analysis are described previously (Batra et al, 2021[1]). In total, 168 patients were included in the analysis (nonlesional = 168, LP = 30, AD = 48, and psoriasis = 90). The accession number is GSE154200.

Cytoscape gene network analysis

Protein–protein interaction network analysis was performed using the STRING software and subsequently visualized in Cytoscape. Gene expression data were used on the basis of Batra et al (2021[1]). More specifically, DAPK1 was used as input protein to generate a protein–protein interaction network on the basis of the following settings and filtering criteria:

- Settings for filtering interactions:
  - Active interaction sources included: experiments, databases, text mining (ie, literature based), and coexpression;
  - Minimum required interaction score of 0.40 (meaning medium confidence threshold); and
  - Disconnected nodes are filtered out.
- Network nodes represent proteins, whereas edges represent protein–protein interactions, with line thickness representing edge confidence (interaction confidence) with following range: from low (0.15), medium (0.40), high (0.70), to highest (0.90).
- Pathway analysis with K-means clustering yielding 3 clusters
  - Dotted lines represent interactions between the different clusters.
  - Blue cluster denotes autophagy.
  - Red cluster denotes apoptosis.
  - Green cluster denotes regulatory proteins involved in different cell death pathways.

Generation of LP-TCS

Lesional T cells of patients were isolated from freshly taken skin biopsies (LP, n = 8) cultivated in RPMI 1640 medium supplemented with 5% human serum, 0.1 mM nonessential amino acid, 2 mM L-glutamine, 1 mM sodium pyruvate, and 100 U/ml penicillin/streptomycin at 37 °C and 5% carbon dioxide. The samples were then placed in 24-well plates with the described medium containing 60 U/ml IL-2. The same number of emigrated T cells for all 3 diseases was expanded with a-CD3 and a-CD28 stimulation (0.75 μg/ml each) as previously described (Lauffer et al, 2018). Cells and supernatants were harvested and used for further experiments.

ELISA

IL-32 protein levels in LP-TCS were determined with an IL-32 ELISA, according to the manufacturer's instructions (R&D System, DY3040-05). An IL-1ß (BD, AB_2869109) and IL-18 (R&D, DY318-05) ELISA was used to determine protein concentration in keratinocyte supernatants.

LUMINEX

The Bio-Plex Pro Human Cytokine 27-plex Assay kit (Bio-Rad Laboratories) was used for measurement of concentration of different cytokines in cell-free T cell supernatants of LP T cells, according to the manufacturer's instrcutions.

Immunohistochemistry

After fixing skin samples in 3.5–3.9% formalin and embedding in paraffin, 3.5-μm sections were prepared. The sections were dewaxed at 65 °C for 20 minutes and rehydrated. After that, heat-induced epitope retrieval in citrate buffer was performed for 7 minutes in citrate buffer. Then, the slides were blocked with peroxidase for 15 minutes, and the Permanent AP Red was used for staining. The primary antibody DAPK1 (Thermo Fisher Scientific, PA5-83502, 1:50) was diluted in antibody diluent and incubated overnight at 4 °C. ZytoChem-Plus AP Polymer-Kit was used for visualization of the antibody, and counterstaining was performed with hematoxylin blue. Slides were fixed, mounted, and imaged under an EVOS M5000 microscope.

Three-dimensional skin models

A total of 0.25×10^6 primary human keratinocytes were added to a collagen-coated (Collagen Type I, Sigma-Aldrich, 1% in PBS) polycarbonate membrane insert (Millipore, PIHP01250) in DermaLife Basal Medium supplemented with the DermaLife K LifeFactor Kit and 1.5 mM calcium chloride. The cells were incubated at 37 °C and 5% carbon dioxide for 48 hours before performing air lift. After air lift, 50 μg/ml vitamin C (Sigma-Aldrich) was additionally added to the sounding medium. Medium exchange was performed every 2 days for at least another 10 days. Stimulation with and without the LP-TCS in the DermaLife k LifeFactor Kit and 1.5 mM calcium chloride without hydrocortisone was performed for 72 hours as described in Lauffer et al (2018). After that, the models were cut out, fixed in 4% formaldehyde, and embedded in paraffin. Finally, 3.5-μm slides were cut, and H&E staining was performed. The number of dead cells was counted blindly by 2 independent investigators.

Viability assay

The CellTiter 96 Aqueous Non-Radioactive Cell Proliferation Assay was used to check for cell viability, according to the manufacturer's instructions. The keratinocytes were stimulated for 24 hours with the LP-TCS diluted 1–10 as well as 1 μM SMAC (LC Laboratories, number B-9135) in the DermaLife K LifeFactor Kit, and viability was compared between the noRNP cells and *DAPK1* KO cells.

Cultivation of keratinocytes

Primary human keratinocytes were obtained by suction blister (Eyerich et al, 2019) and cultured in DermaLife Basal Medium, which was supplemented with the DermaLife K LifeFactor Kit, at 37 °C and 5% carbon dioxide. The 1.5E05 cells were cultured in 6-well plates for 4 days. After starving the cells in DermaLife Basal Medium without supplements for 5 hours, they were stimulated with different cytokines for 48 hours for western blot analysis and 16 hours for RNA analysis in supplemented DermaLife Basal Medium without hydrocortisone. The keratinocytes were stimulated with the following antibodies: IFN-γ (50 ng/ml), TNF (50 ng/ml) and IFN-α (50 ng/ml), IL-32γ (50 ng/ml and 100 ng/ml), IL-17A (50 ng/ml), IL-13 (50 ng/ml) (all from R&D systems), and IL-4 (50 ng/ml, Miltenyi).

Western blot

Cultured cells were lysed using RIPA lysis buffer (Santa Cruz Biotechnology), which was supplemented with 2 mM phenylmethylsulfonyl fluoride (1:100), 1 mM sodium orthovanadate (1:100), and a proteinase inhibitor cocktail (1:75). Protein concentration was determined by a BCA protein assay (Thermo Fisher Scientific). Equal protein concentrations were mixed with Laemmli loading buffer and loaded onto a Bolt 4–12% Bis-TrisPlus Gel (Invitrogen). Western blot analysis was performed using enhanced chemiluminescence. The following antibodies were used: DAPK1 (Cell Signaling Technology, number 3008, 1:1000) dissolved in 5% milk, RIPK3 (Abcam, ab62344, 1:2000), PARP (Cell Signaling Technology, number 9532, 1:1000), BAX (Cell Signaling Technology, number 2772, 1:1000), and phosphorylated DAPK1 (Ser734) (Thermo Fisher Scientific, PA5-105872, 1:500) dissolved in BSA followed by either antirabbit horseradish peroxidase (Santa Cruz, 1:10,000) or antimouse horseradish peroxidase (Jackson Laboratories, 1:10,000) dissolved in BSA. For quantification, DAPK1 expression was normalized to the housekeeper before analysis of intensity.

qPCR

RNA from cultured cells was extracted using the miRNeasy Mini Plus Kit (Qiagen). After that, cDNA was synthesized and transcribed from 500 ng of total RNA using the High-Capacity cDNA Reverse Transcript Amplification Kit (Applied Biosystems), according to the manufacturer's instructions. Real-time PCR was performed using Fast Start SYBR Green Master Mix (Roche) and monitored with the ViiA7 Real Time PCR machine (Applied Biosystems). Primers of the genes of interest were designed with National Center for Biotechnology Information Primer Blast and synthesized by Metabion. Gene expression was normalized to the housekeeping gene *18S*. Expression results were analyzed using the ΔΔCT method. The following primers were used: *18S* (forward GTA ACC CGT TGA ACC CCA TT; reverse CCA TCC AAT CGG TAG TAG CG), *RIPK3* (forward CAG ATT CGA TGG CCC AAC CT; rev TTG TCT CTC AGC CCC CTG AT), *MLKL* (forward GTC CGG TAC AGT CAG CAG AG; reverse ATT TTC CAT GCT TCG CGC C), *BAX* (forward CCC GAG AGG TCT TTT TCC GAG; reverse CCA GCC CAT GAT GGT TCT GAT), *Bcl-2* (forward GGT GGG GTC ATG TGT GTG G; reverse CGG TTC AGG TAC TCA GTC ATC C), *CXCL9* (forward GAG TGC AAG GAA CCC CAG TAG; reverse GGT GGA TAG TCC CTT GGT TGG), *CXCL10* (forward AAC CTC CAG TCT CAG CAC CA; reverse GAG AGA GGT ACT CCT TGA ATG CC), *CXCL11* (forward TTG TTC AAG GCT TCC CCA TGT T; reverse CAC TTT CAC TGC TTT TAC CCC A), *IL1ß* (forward AAG CCC TTG CTG TAG TGG TG; reverse GAA GCT GAT GGC CCT AAA CA), *IL32* (forward GAC AGT GGC GGC TTA TTA TGA G; reverse CCT CGG CAC CGT AAT CCA T), *TNF* (forward TGT TGT AGC AAA CCC TCA AGC; reverse ATG AGG TAC AGG CCC TCT GA), *ICAM1* (forward CCT CAC CGT GTA CTG GAC TC; reverse GGG TAA GGT TCT TGC CCA CT), and *CCL2* (forward TCC CAA AGA AGC TGT GAT CTT CA; reverse TTT GCT TGT CCA GGT GGT CC).

Histological score

The strength of ID of every sample was rated 0–3 by 2 independent dermatopathologists on the basis of the amount of infiltrating immune cells and the number of epidermal dyskeratosis.

Statistical analysis

Data were visualized with GraphPad Prism 9.0 and analyzed for significance with either unpaired or paired *t*-test or 1-way ANOVA as indicated in the figure legend. The significance level was defined as $*P \leq .05$, $**P \leq .01$, $***P \leq .001$, and $****P \leq .0001$.

DATA AVAILABILITY STATEMENT

All data are available from the corresponding author upon reasonable request. Datasets related to this article can be found at https://www.ncbi.nlm.nih.gov/geo/query/acc.cgi?acc=GSE154200 (Batra et al, 2021[1]) and https://www.ncbi.nlm.nih.gov/geo/query/acc.cgi?acc=GSE206391 (Schäbitz et al, 2022), hosted at Gene Expression Omnibus.

CONFLICT OF INTEREST

The authors state no conflict of interest.

ACKNOWLEDGMENTS

We thank Jana Sänger for excellent technical support. The study used samples of the biobank Biederstein of the Department of Dermatology, Technical University Munich. This project was funded by the Deutsche Forschungsgemeinschaft (German Research Foundation) RTG2668 project A3 (project number 435874434) and the Doctoral Program Translational Medicine of the School of Medicine and Health of the Technical University of Munich.

AUTHOR CONTRIBUTIONS

Conceptualization: NK, MM, MJ, FL; Funding Acquisition: FL, SE; Methodology: NK, MJ, MM, CH, SW, JE; Project Administration: NK, FL; Supervision: FL, SE; Visualization: NK, MJ, PS, MM; Writing – Original Draft Preparation: NK, MM, FL; Writing - Review and editing: NK, FL, SE, MM, MJ, JE, TB, CBS-W, KE

SUPPLEMENTARY MATERIAL

Supplementary material is linked to the online version of the paper at www.jidonline.org, and at https://doi.org/10.1016/j.jid.2024.11.017.

REFERENCES

Barathan M, Gopal K, Mohamed R, Ellegård R, Saeidi A, Vadivelu J, et al. Chronic hepatitis C virus infection triggers spontaneous differential expression of biosignatures associated with T cell exhaustion and apoptosis signaling in peripheral blood mononucleocytes. Apoptosis 2015;20:466–80.

Boehncke WH, Schön MP. Psoriasis. Lancet 2015;386:983–94.

Brunner PM, Silverberg JI, Guttman-Yassky E, Paller AS, Kabashima K, Amagai M, et al. Increasing comorbidities suggest that atopic dermatitis is a systemic disorder. J Invest Dermatol 2017;137:18–25.

Chen D, Zhou XZ, Lee TH. Death-associated protein kinase 1 as a promising drug target in cancer and Alzheimer's disease. Recent Pat Anticancer Drug Discov 2019;14:144–57.

Chen L, Zhang X, Ou Y, Liu M, Yu D, Song Z, et al. Advances in RIPK1 kinase inhibitors. Front Pharmacol 2022;13:976435.

Dickman J, Howell M, Hoopes R, Wang Y, Dickerson TJ, Bottomley M, et al. Insights into Lichen Planus pigmentosus inversus using minimally invasive dermal patch and whole transcriptome analysis. J Clin Investig Dermatol 2022;10. https://doi.org/10.13188/2373-1044.1000077.

Eyerich K, Brown SJ, Perez White BE, Tanaka RJ, Bissonette R, Dhar S, et al. Human and computational models of atopic dermatitis: a review and perspectives by an expert panel of the International Eczema Council. J Allergy Clin Immunol 2019;143:36–45.

Eyerich K, Eyerich S. Immune response patterns in non-communicable inflammatory skin diseases. J Eur Acad Dermatol Venereol 2018;32:692–703.

Fiocco Z, Kupf S, Patzak L, Kämmerer T, Pumnea T, French LE, et al. Quality of life and psychopathology in Lichen Planus: a neglected disease burden. Acta Derm Venereol 2021;101:adv00619.

Freund L, Oehrl S, Schwingen J, Haeberle S, Döbel T, Lee PDH, et al. IFNγ causes keratinocyte necroptosis in acute graft-versus-host disease. J Invest Dermatol 2023;143:1746–56.e9.

Gandesiri M, Chakilam S, Ivanovska J, Benderska N, Ocker M, Di Fazio P, et al. DAPK plays an important role in panobinostat-induced autophagy and commits cells to apoptosis under autophagy deficient conditions [published correction appears in Apoptosis 2016;21:671–4]. Apoptosis 2012;17:1300–15.

Khoury MK, Gupta K, Franco SR, Liu B. Necroptosis in the pathophysiology of disease. Am J Pathol 2020;190:272–85.

Kim SK, Kim WJ, Yoon JH, Ji JH, Morgan MJ, Cho H, et al. Upregulated RIP3 expression potentiates MLKL phosphorylation-mediated programmed necrosis in toxic epidermal necrolysis. J Invest Dermatol 2015;135:2021–30.

Lai MZ, Chen RH. Regulation of inflammation by DAPK. Apoptosis 2014;19:357–63.

Lauffer F, Jargosch M, Krause L, Garzorz-Stark N, Franz R, Roenneberg S, et al. Type I immune response induces keratinocyte necroptosis and is associated with interface dermatitis. J Invest Dermatol 2018;138:1785–94.

Lee CW, Leu SJ, Tzeng RY, Wang SF, Tsai SC, Sun KH, et al. Latent membrane protein 1 of Epstein-Barr virus regulates death-associated protein kinase 1 in lymphoblastoid cell line. Virology 2011;413:19–25.

Li T, Wu YN, Wang H, Ma JY, Zhai SS, Duan J. Dapk1 improves inflammation, oxidative stress and autophagy in LPS-induced acute lung injury via p38MAPK/NF-κB signaling pathway. Mol Immunol 2020;120:13–22.

Schäbitz A, Hillig C, Mubarak M, Jargosch M, Farnoud A, Scala E, et al. Spatial transcriptomics landscape of lesions from non-communicable inflammatory skin diseases. Nat Commun 2022;13:7729.

Schruf E, Biermann MH, Jacob J, Häckl D, Reinhardt M, Hertl M, et al. Lichen planus in Germany - epidemiology, treatment, and comorbidity. A retrospective claims data analysis. J Dtsch Dermatol Ges 2022;20:1101–10.

Shao S, Tsoi LC, Sarkar MK, Xing X, Xue K, Uppala R, et al. IFN-γ enhances cell-mediated cytotoxicity against keratinocytes via JAK2/STAT1 in lichen planus. Sci Transl Med 2019;11:eaav7561.

Singh P, Ravanan P, Talwar P. Death associated protein kinase 1 (DAPK1): A regulator of apoptosis and autophagy. Front Mol Neurosci 2016;23(9):46.

Sontheimer RD. Lichenoid tissue reaction/interface dermatitis: clinical and histological perspectives. J Invest Dermatol 2009;129:1088–99.

Steinmann S, Kunze P, Hampel C, Eckstein M, Bertram Bramsen J, Muenzner JK, et al. DAPK1 loss triggers tumor invasion in colorectal tumor cells. Cell Death Dis 2019;10:895.

Turner-Brannen E, Choi KY, Arsenault R, El-Gabalawy H, Napper S, Mookherjee N. Inflammatory cytokines IL-32 and IL-17 have common signaling intermediates despite differential dependence on TNF-receptor 1. J Immunol 2011;186:7127–35.

Wang S, Su H, Feng P, Deng W, Su C, Wu Y, et al. Loss of death-associated protein kinase 1 in human bone marrow mesenchymal stem cells decreases immunosuppression of CD4+ T cells. J Int Med Res 2020a;48:300060520933453.

Wang Y, Fang X, Yang Y, Chen L, Xiong W, Song L, et al. Death-associated protein kinase 1 promotes alveolar epithelial cell apoptosis and ventilator-induced lung injury through P53 pathway. Shock 2022;57:140–50.

Wang Y, Yang Y, Chen L, Xiong W, Song L, Li B, et al. Death-associated protein kinase 1 mediates ventilator-induced lung injury in mice by promoting alveolar epithelial cell apoptosis. Anesthesiology 2020b;133:905–18.

Wei Z, Li P, He R, Liu H, Liu N, Xia Y, et al. DAPK1 (death associated protein kinase 1) mediates mTORC1 activation and antiviral activities in $CD8^+$ T cells. Cell Mol Immunol 2021;18:138–49.

Wenzel J, Peters B, Zahn S, Birth M, Hofmann K, Küsters D, et al. Gene expression profiling of lichen planus reflects CXCL9+-mediated inflammation and distinguishes this disease from atopic dermatitis and psoriasis. J Invest Dermatol 2008;128:67–78.

Wenzel J, Tüting T. An IFN-associated cytotoxic cellular immune response against viral, self-, or tumor antigens is a common pathogenetic feature in "interface dermatitis". J Invest Dermatol 2008;128:2392–402.

Xie JY, Chen PC, Zhang JL, Gao ZS, Neves H, Zhang SD, et al. The prognostic significance of DAPK1 in bladder cancer. PLoS One 2017;12:e0175290.

Yoo HJ, Byun HJ, Kim BR, Lee KH, Park SY, Rho SB. DAPk1 inhibits NF-κB activation through TNF-α and INF-γ-induced apoptosis. Cell Signal 2012;24:1471–7.

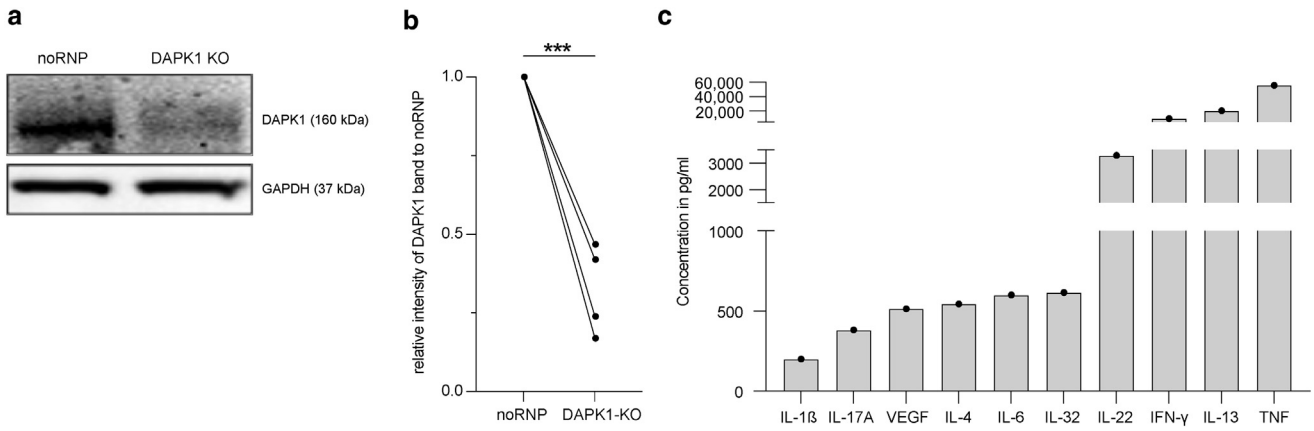

Supplementary Figure S1. DAPK1 knock out efficiency and characterization of lichen planus-derived T cell supernatant. (**a**) Representative picture of western blot analysis of DAPK1 in noRNP compared with that in *DAPK1*-KO keratinocytes upon stimulation with IFN-γ + TNF for KO efficiency validation. (**b**) Quantification of western blot analysis of DAPK1 expression in noRNP compared with that in *DAPK1*-KO keratinocytes upon stimulation with IFN-γ + TNF for KO efficiency validation (n = 4). (**c**) Protein concentration in pg/ml of different cytokines measured in LP-TCS with LUMINEX analysis or ELISA. Paired *t*-test was used for significance analysis between noRNP and *DAPK1* KO. ****$P < .0001$. KO, knockout; LP-TCS, lichen planus–derived supernatant T cell.

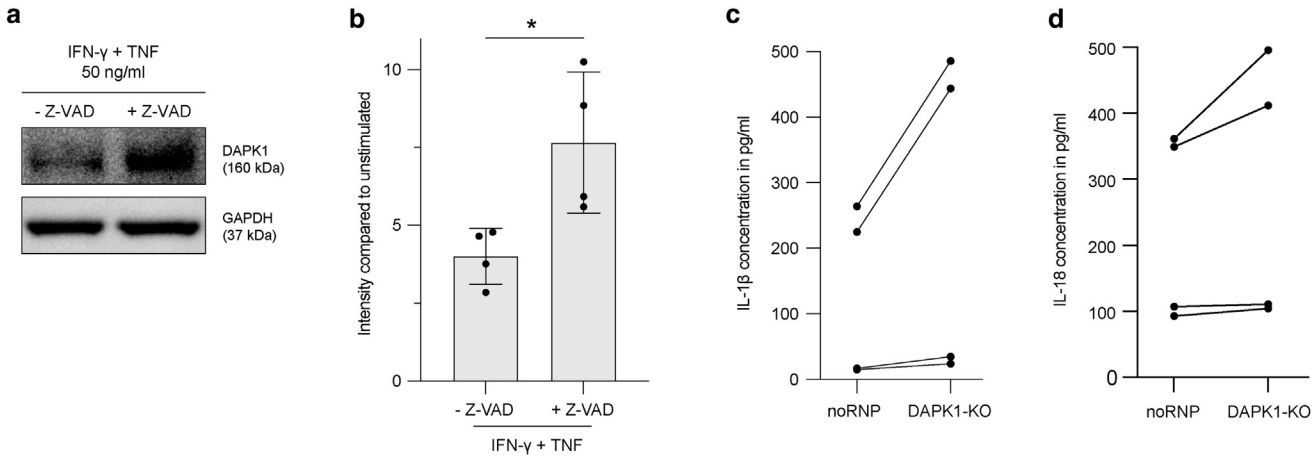

Supplementary Figure S2. DAPK1 is induced after inhibition of apoptosis using Z-VAD. **(a)** Representative picture of western blot analysis of DAPK1 expression in keratinocytes after stimulation with IFN-γ + TNF (50 ng/ml) under normal (− ZVAD) or necroptotic (+ ZVAD) conditions. (**b**) Quantification of western blot analysis of DAPK1 levels in keratinocytes after stimulation with IFN-γ + TNF (50 ng/ml) under normal (− ZVAD) or necroptotic (+ ZVAD) conditions (n = 4) (**c, d**) Absolute (**c**) IL-1β or (**d**) IL-18 concentrations in noRNP compared with that in *DAPK1*-KO keratinocytes (n = 4) upon stimulation with lesional LP-TCS for 24 h. Paired *t*-test was used for significance analysis between IFN-γ + TNF with or without ZVAD and noRNP and *DAPK1* KO. *$P < .05$. h, hour; KO, knockout; LP-TCS, lichen planus–derived supernatant T cell.

Supplementary Table S1. Patient's Characteristics for the Bulk RNA Sequencing Cohort of LP (n = 30), AD (n = 48), and Psoriasis (n = 90) Skin Lesions

Donor ID	RNA-Sequencing Sample Name		Sex	Age, y	Diagnosis
	lesional	Nonlesional			
10005	MUC2860	MUC2861	M	44.8	LP
10009	MUC2862	MUC2863	F	79.3	LP
10016	MUC2864	MUC2865	F	43.9	LP
10053	MUC2866		M	51.1	LP
10069	MUC2868	MUC2869	F	65.3	LP
10074	MUC2870	MUC2871	M	71.6	LP
10075	MUC2872	MUC2873	F	51.7	LP
10076	MUC2874	MUC2875	F	75.5	LP
10104	MUC2876	MUC2877	M	43.2	LP
10109	MUC2878	MUC2879	M	59.9	LP
10113	MUC2880	MUC2881	M	65.2	LP
10174	MUC2882	MUC2883	F	39.0	LP
10212	MUC3757	MUC3758	F	74.0	LP
10317	MUC4251	MUC4252	M	61.8	LP
10318	MUC3741	MUC3742	F	54.5	LP
10340	MUC3739	MUC3740	F	65.2	LP
10347	MUC2955	MUC2956	F	78.7	LP
10382	MUC3733	MUC3734	M	63.9	LP
10422	MUC3709	MUC3710	M	54.8	LP
10435	MUC3701	MUC3702	F	33.8	LP
10458	MUC4295	MUC4296	F	57.6	LP
10492	MUC4309	MUC4310	F	84.7	LP
10496	MUC4311	MUC4312	M	56.2	LP
10532	MUC4323	MUC4324	F	70.6	LP
10576	MUC7271	MUC7272	F	54.7	LP
10613	MUC7297	MUC7298	M	28.9	LP
10622	MUC7299	MUC7300	M	72.2	LP
10640	MUC7259		F	54.0	LP
10687	MUC7311	MUC7312	F	65.8	LP
10705	MUC7351	MUC7352	M	43.2	LP
n = 30	n = 30	n = 28	F: 25	56.1	
			M: 16	± 15.4	
10004	MUC2676	MUC2677	F	27.9	AD
10007	MUC2678	MUC2679	M	27.5	AD
10020	MUC2680	MUC2681	F	22.5	AD
10025	MUC2684	MUC2685	M	23.6	AD
10035	MUC2688	MUC2689	F	51.5	AD
10043	MUC2690	MUC2691	M	72.3	AD
10063	MUC2692	MUC2693	F	27.1	AD
10071	MUC2697	MUC2698	F	79.3	AD
10085	MUC2703	MUC2704	F	35.1	AD
10089	MUC2707	MUC2708	M	62.3	AD
10091	MUC2777	MUC2778	M	81.6	AD
10137	MUC2711	MUC2712	M	29.0	AD
10146	MUC2717	MUC2718	M	25.9	AD
10147	MUC2719	MUC2720	M	25.3	AD
10149	MUC2836	MUC2837	F	87.0	AD
10175	MUC2733	MUC2734	M	23.2	AD
10248	MUC7378	MUC7379	F	53.1	AD
10264	MUC3753	MUC3754	M	57.3	AD
10269	MUC7381		M	54.2	AD
10294	MUC2943	MUC2944	M	50.0	AD
10320	MUC4253	MUC4254	M	47.5	AD
10321	MUC2945	MUC2946	M	79.6	AD
10350	MUC4259	MUC4260	W	73.5	AD
10367	MUC2951	MUC2952	M	68.5	AD

(*continued*)

Supplementary Table S1. Continued

Donor ID	RNA-Sequencing Sample Name	Sex	Age, y	Diagnosis	
10393	MUC4279	MUC4280	M	39.4	AD
10401	MUC4281	MUC4282	M	77.7	AD
10416	MUC4285	MUC4286	M	61.8	AD
10442	MUC4287	MUC4288	M	22.8	AD
10452	MUC4291	MUC4292	M	51.2	AD
10462	MUC4299	MUC4300	F	66.4	AD
10464	MUC4301	MUC4302	M	56.7	AD
10498	MUC4313	MUC4314	M	74.2	AD
10570	MUC7277	MUC7278	F	45.0	AD
10654	MUC7237	MUC7238	M	56.8	AD
10655	MUC7342	MUC7343	M	53.7	AD
10664	MUC7389	MUC7390	F	74.0	AD
10671	MUC7320		F	23.9	AD
10682	MUC7333	MUC7334	F	21.5	AD
13237	MUC2898	MUC2899	M	56.0	AD
16083	MUC2917	MUC2918	M	31.5	AD
24627	MUC2893	MUC2894	F	47.6	AD
28093	MUC2914	MUC2915	F	26.2	AD
37685	MUC2895	MUC2896	M	38.7	AD
48724	MUC2906	MUC2907	M	49.6	AD
51694	MUC2900	MUC2901	M	56.0	AD
57856	MUC2911	MUC2912	M	36.8	AD
71982	MUC2903	MUC2904	M	41.6	AD
83239	MUC2908	MUC2909	M	33.1	AD
n = 48	n = 48	n = 46	F: 16	48.5	
			M: 32	± 19.4	
10002	MUC2737	MUC2738	F	18.3	Psoriasis
10006	MUC2739	MUC2740	M	42.7	Psoriasis
10013	MUC2741	MUC2742	M	50.3	Psoriasis
10019	MUC2743	MUC2744	M	59.3	Psoriasis
10030	MUC2745	MUC2746	M	38.3	Psoriasis
10033	MUC2747	MUC2748	M	67.6	Psoriasis
10034	MUC2749	MUC2750	F	67.5	Psoriasis
10036	MUC2751	MUC2752	M	52.6	Psoriasis
10046	MUC2753	MUC2754	M	54.8	Psoriasis
10049	MUC2755	MUC2756	M	45.8	Psoriasis
10051	MUC2757	MUC2758	F	42.2	Psoriasis
10052	MUC2759	MUC2760	F	90.6	Psoriasis
10056	MUC2761	MUC2762	M	23.0	Psoriasis
10058	MUC2763	MUC2764	F	70.3	Psoriasis
10060	MUC2765	MUC2766	M	52.9	Psoriasis
10064	MUC2767	MUC2768	F	92.2	Psoriasis
10067	MUC2769	MUC2770	M	42.3	Psoriasis
10072	MUC2771	MUC2772	F	31.7	Psoriasis
10078	MUC7393		M	51.4	Psoriasis
10079	MUC2699	MUC2700	M	24.7	Psoriasis
10083	MUC2773	MUC2774	F	41.8	Psoriasis
10103	MUC2779	MUC2780	M	55.2	Psoriasis
10119	MUC2709	MUC2710	F	57.0	Psoriasis
10128	MUC2781	MUC2782	F	53.5	Psoriasis
10133	MUC2783	MUC2784	M	63.7	Psoriasis
10136	MUC2785	MUC2786	F	67.5	Psoriasis
10138	MUC2787	MUC2788	F	68.6	Psoriasis
10153	MUC2789	MUC2790	F	46.9	Psoriasis
10154	MUC2791	MUC2792	F	55.4	Psoriasis
10158	MUC2723	MUC2724	M	55.4	Psoriasis

(*continued*)

Supplementary Table S1. Continued

Donor ID	RNA-Sequencing Sample Name	Sex	Age, y	Diagnosis	
10159	MUC2725	MUC2726	F	53.4	Psoriasis
10171	MUC2793	MUC2794	M	57.0	Psoriasis
10172	MUC2795	MUC2796	F	91.0	Psoriasis
10177	MUC2797	MUC2798	M	51.6	Psoriasis
10195	MUC2799	MUC2800	M	47.4	Psoriasis
10198	MUC2801	MUC2802	M	54.3	Psoriasis
10199	MUC2803	MUC2804	F	44.1	Psoriasis
10200	MUC2805	MUC2806	M	38.5	Psoriasis
10203	MUC2807	MUC2808	M	49.7	Psoriasis
10206	MUC2809	MUC2810	F	27.6	Psoriasis
10208	MUC2811	MUC2812	F	65.8	Psoriasis
10210	MUC2813	MUC2814	F	50.7	Psoriasis
10211	MUC2815	MUC2816	M	39.4	Psoriasis
10227	MUC2840	MUC2841	M	54.6	Psoriasis
10233	MUC2817	MUC2818	M	58.4	Psoriasis
10235	MUC2819	MUC2820	F	42.8	Psoriasis
10239	MUC2821	MUC2822	F	88.7	Psoriasis
10242	MUC7392	MUC7393	F	65.9	Psoriasis
10249	MUC7380	MUC7381	M	72.7	Psoriasis
10282	MUC3749	MUC3750	M	38.7	Psoriasis
10297	MUC4241	MUC4242	F	66.6	Psoriasis
10298	MUC4243	MUC4244	M	71.4	Psoriasis
10307	MUC4245	MUC4246	M	46.4	Psoriasis
10327	MUC4255	MUC4256	M	44.1	Psoriasis
10343	MUC4257	MUC4258	M	76.6	Psoriasis
10354	MUC4261	MUC4262	M	74.7	Psoriasis
10369	MUC4265	MUC4266	F	51.6	Psoriasis
10372	MUC4267	MUC4268	M	78.2	Psoriasis
10379	MUC4271	MUC4272	F	68.8	Psoriasis
10384	MUC4273	MUC4274	M	47.1	Psoriasis
10386	MUC4275	MUC4276	M	81.8	Psoriasis
10419	MUC3713	MUC3714	F	73.7	Psoriasis
10429	MUC3705	MUC3706	M	60.9	Psoriasis
10456	MUC4293	MUC4294	M	33.9	Psoriasis
10461	MUC4297	MUC4298	F	53.8	Psoriasis
10465	MUC4303	MUC4304	M	49.8	Psoriasis
10482	MUC3671	MUC3672	F	58.8	Psoriasis
10489	MUC4307	MUC4308	F	84.6	Psoriasis
10542	MUC7382		M	57.3	Psoriasis
10562	MUC7383	MUC7384	F	42.5	Psoriasis
10574	MUC7386	MUC7387	M	39.3	Psoriasis
10578	MUC7376	MUC7377	M	51.9	Psoriasis
10590	MUC7371	MUC7372	M	61.7	Psoriasis
10602	MUC7367	MUC7368	M	55.7	Psoriasis
10609	MUC7366	MUC7367	F	73.4	Psoriasis
10615	MUC7363	MUC7364	M	66.9	Psoriasis
10616	MUC7362	MUC7363	M	67.3	Psoriasis
10620	MUC7359	MUC7360	M	36.9	Psoriasis
10626	MUC7355	MUC7356	M	68.1	Psoriasis
10630	MUC7354	MUC7355	F	58.2	Psoriasis
10631	MUC7301	MUC7302	M	24.6	Psoriasis
10633	MUC7305	MUC7306	F	37.3	Psoriasis
10645	MUC7350	MUC7351	F	60.0	Psoriasis
10646	MUC7348	MUC7349	M	58.6	Psoriasis
10649	MUC7345	MUC7346	M	53.6	Psoriasis
10650	MUC7344	MUC7345	F	43.5	Psoriasis
10656	MUC7339	MUC7340	F	48.5	Psoriasis

(*continued*)

Supplementary Table S1. Continued

Donor ID	RNA-Sequencing Sample Name	Sex	Age, y	Diagnosis	
10665	MUC7338	MUC7339	M	25.8	Psoriasis
10668	MUC7336	MUC7337	F	25.1	Psoriasis
10691	MUC7330	MUC7331	M	46.8	Psoriasis
n = 90	n = 90	n = 88	F: 38 M: 52	54.5 ± 16.1	

Abbreviations: AD, atopic dermatitis; F, female; ID, identification; LP, lichen planus; M, male.

Supplementary Table S2. Enrichment KEGG

Term ID	Term Description	Observed Gene Count	Background Gene Count	Strength	False Discovery Rate	Matching Proteins in Your Network (IDs)
hsa04621	NOD-like receptor signaling pathway	11	174	1.71	2.98e-14	9606.ENSP00000037243, 9606.ENSP00000215832, 9606.EN/SP00000216160, 9606.ENSP00000216274, 9606.ENSP00000263025, 9606.ENSP00000302564, 9606.ENSP00000351273, 9606.ENSP00000358072,9606.ENSP0000
hsa04140	Autophagy - animal	10	130	1.8	7.59e-14	9606.ENSP00000037243, 9606.ENSP00000215832, 9606.ENSP00000247178, 9606.ENSP00000263025, 9606.ENSP00000283290, 9606.ENSP00000302564, 9606.ENSP00000349205, 9606.ENSP00000358072,9606.ENSP0000
hsa05131	Shigellosis	11	218	1.61	1.07e-13	9606.ENSP00000037243, 9606.ENSP00000162749, 9606.ENSP00000215832, 9606.ENSP00000216160, 9606.ENSP00000247178, 9606.ENSP00000263025, 9606.ENSP00000302564, 9606.ENSP00000349205,9606.ENSP0000
hsa05167	Kaposi sarcoma −associated herpesvirus infection	10	187	1.64	1.23e-12	9606.ENSP00000037243, 9606.ENSP00000162749, 9606.ENSP00000215832, 9606.ENSP00000247178, 9606.ENSP00000263025, 9606.ENSP00000272298, 9606.ENSP00000283290, 9606.ENSP00000311032,9606.ENSP0000
hsa05145	Toxoplasmosis	8	105	1.79	4.36e-11	9606.ENSP00000162749, 9606.ENSP00000215832, 9606.ENSP00000216160, 9606.ENSP00000263025, 9606.ENSP00000302564, 9606.ENSP00000311032, 9606.ENSP00000351273, 9606.ENSP00000360242
hsa04668	TNF signaling pathway	8	112	1.77	5.94e-11	9606.ENSP00000162749, 9606.ENSP00000215832, 9606.ENSP00000216160, 9606.ENSP00000216274, 9606.ENSP00000263025, 9606.ENSP00000311032, 9606.ENSP00000351273, 9606.ENSP00000360266
hsa05170	HIV infection	9	204	1.56	9.77e-11	9606.ENSP00000162749, 9606.ENSP00000215832, 9606.ENSP00000216160, 9606.ENSP00000263025, 9606.ENSP00000272298, 9606.ENSP00000302564, 9606.ENSP00000311032, 9606.ENSP00000351273,9606.ENSP0000
hsa04210	Apoptosis	8	132	1.69	1.56e-10	9606.ENSP00000162749, 9606.ENSP00000215832, 9606.ENSP00000263025, 9606.ENSP00000302564, 9606.ENSP00000311032, 9606.ENSP00000351273, 9606.ENSP00000360242, 9606.ENSP00000360266
hsa05130	Pathogenic Escherichia coli infection	8	187	1.54	2.00e-09	9606.ENSP00000162749, 9606.ENSP00000215832, 9606.ENSP00000216160, 9606.ENSP00000263025, 9606.ENSP00000311032, 9606.ENSP00000340944, 9606.ENSP00000351273, 9606.ENSP00000360266
hsa05132	Salmonella infection	8	209	1.49	4.23e-09	9606.ENSP00000162749, 9606.ENSP00000215832, 9606.ENSP00000216160, 9606.ENSP00000216274, 9606.ENSP00000263025, 9606.ENSP00000311032, 9606.ENSP00000351273, 9606.ENSP00000360266
hsa05010	Alzheimer disease	9	355	1.32	7.47e-09	9606.ENSP00000162749, 9606.ENSP00000215832, 9606.ENSP00000247178, 9606.ENSP00000263025, 9606.ENSP00000272298, 9606.ENSP00000290277, 9606.ENSP00000311032, 9606.ENSP00000349205,9606.ENSP0000
hsa05200	Pathways in cancer	10	517	1.2	7.47e-09	9606.ENSP00000215832, 9606.ENSP00000263025, 9606.ENSP00000272298, 9606.ENSP00000290277, 9606.ENSP00000302564, 9606.ENSP00000311032, 9606.ENSP00000351273, 9606.ENSP00000360242,9606.ENSP0000
hsa01524	Platinum drug resistance	6	70	1.84	9.17e-09	9606.ENSP00000215832, 9606.ENSP00000263025, 9606.ENSP00000302564, 9606.ENSP00000311032, 9606.ENSP00000351273, 9606.ENSP00000360242
hsa04136	Autophagy - other	5	29	2.15	1.15e-08	9606.ENSP00000037243, 9606.ENSP00000283290, 9606.ENSP00000349205, 9606.ENSP00000358072, 9606.ENSP00000425107
hsa04215	Apoptosis - multiple species	5	30	2.13	1.26e-08	9606.ENSP00000162749, 9606.ENSP00000302564, 9606.ENSP00000311032, 9606.ENSP00000351273, 9606.ENSP00000360242

(*continued*)

Supplementary Table S2. Continued

Term ID	Term Description	Observed Gene Count	Background Gene Count	Strength	False Discovery Rate	Matching Proteins in Your Network (IDs)
hsa05161	Hepatitis B	7	159	1.55	1.78e-08	9606.ENSP00000215832, 9606.ENSP00000216160, 9606.ENSP00000263025, 9606.ENSP00000290277, 9606.ENSP00000311032, 9606.ENSP00000351273, 9606.ENSP00000360266
hsa04010	MAPK signaling pathway	8	288	1.35	2.91e-08	9606.ENSP00000162749, 9606.ENSP00000215832, 9606.ENSP00000216160, 9606.ENSP00000263025, 9606.ENSP00000279488, 9606.ENSP00000290277, 9606.ENSP00000311032, 9606.ENSP00000360266
hsa04625	C-type lectin receptor signaling pathway	6	102	1.68	5.66e-08	9606.ENSP00000215832, 9606.ENSP00000263025, 9606.ENSP00000272298, 9606.ENSP00000340944, 9606.ENSP00000351273, 9606.ENSP00000360266
hsa05211	Renal cell carcinoma	5	66	1.79	3.86e-07	9606.ENSP00000215832, 9606.ENSP00000263025, 9606.ENSP00000290277, 9606.ENSP00000340944, 9606.ENSP00000360266
hsa05160	Hepatitis C	6	156	1.5	5.83e-07	9606.ENSP00000162749, 9606.ENSP00000215832, 9606.ENSP00000263025, 9606.ENSP00000290277, 9606.ENSP00000311032, 9606.ENSP00000351273
hsa05133	Pertussis	5	74	1.74	6.01e-07	9606.ENSP00000215832, 9606.ENSP00000263025, 9606.ENSP00000272298, 9606.ENSP00000311032, 9606.ENSP00000360266
hsa05220	Chronic myeloid leukemia	5	75	1.74	6.11e-07	9606.ENSP00000215832, 9606.ENSP00000263025, 9606.ENSP00000290277, 9606.ENSP00000302564, 9606.ENSP00000340944
hsa05152	Tuberculosis	6	168	1.46	7.76e-07	9606.ENSP00000162749, 9606.ENSP00000215832, 9606.ENSP00000263025, 9606.ENSP00000272298, 9606.ENSP00000311032, 9606.ENSP00000351273
hsa05210	Colorectal cancer	5	82	1.7	8.56e-07	9606.ENSP00000215832, 9606.ENSP00000263025, 9606.ENSP00000290277, 9606.ENSP00000311032, 9606.ENSP00000360266
hsa04657	IL-17 signaling pathway	5	92	1.65	1.42e-06	9606.ENSP00000215832, 9606.ENSP00000263025, 9606.ENSP00000311032, 9606.ENSP00000351273, 9606.ENSP00000360266
hsa01522	Endocrine resistance	5	95	1.63	1.59e-06	9606.ENSP00000215832, 9606.ENSP00000216115, 9606.ENSP00000263025, 9606.ENSP00000290277, 9606.ENSP00000360266
hsa05142	Chagas disease	5	99	1.61	1.87e-06	9606.ENSP00000162749, 9606.ENSP00000215832, 9606.ENSP00000263025, 9606.ENSP00000351273, 9606.ENSP00000360266
hsa04620	Toll-like receptor signaling pathway	5	101	1.61	1.98e-06	9606.ENSP00000215832, 9606.ENSP00000216160, 9606.ENSP00000263025, 9606.ENSP00000351273, 9606.ENSP00000360266
hsa05166	Human T-cell leukemia virus 1 infection	6	211	1.37	2.28e-06	9606.ENSP00000162749, 9606.ENSP00000215832, 9606.ENSP00000263025, 9606.ENSP00000302564, 9606.ENSP00000360242, 9606.ENSP00000360266
hsa05163	Human cytomegalovirus infection	6	218	1.35	2.65e-06	9606.ENSP00000162749, 9606.ENSP00000215832, 9606.ENSP00000263025, 9606.ENSP00000272298, 9606.ENSP00000311032, 9606.ENSP00000351273
hsa05219	Bladder cancer	4	41	1.9	2.71e-06	9606.ENSP00000215832, 9606.ENSP00000263025, 9606.ENSP00000290277, 9606.ENSP00000386135
hsa04722	Neurotrophin signaling pathway	5	114	1.55	3.09e-06	9606.ENSP00000215832, 9606.ENSP00000263025, 9606.ENSP00000272298, 9606.ENSP00000340944, 9606.ENSP00000360266
hsa04650	Natural killer cell mediated cytotoxicity	5	121	1.53	3.99e-06	9606.ENSP00000215832, 9606.ENSP00000263025, 9606.ENSP00000290277, 9606.ENSP00000311032, 9606.ENSP00000340944
hsa04380	Osteoclast differentiation	5	122	1.52	4.03e-06	9606.ENSP00000162749, 9606.ENSP00000215832, 9606.ENSP00000216160, 9606.ENSP00000263025, 9606.ENSP00000360266
hsa04068	FoxO signaling pathway	5	127	1.51	4.74e-06	9606.ENSP00000037243, 9606.ENSP00000215832, 9606.ENSP00000263025, 9606.ENSP00000290277, 9606.ENSP00000425107
hsa04371	Apelin signaling pathway	5	131	1.49	5.34e-06	9606.ENSP00000037243, 9606.ENSP00000215832, 9606.ENSP00000263025, 9606.ENSP00000272298, 9606.ENSP00000349205

(*continued*)

Supplementary Table S2. Continued

Term ID	Term Description	Observed Gene Count	Background Gene Count	Strength	False Discovery Rate	Matching Proteins in Your Network (IDs)
hsa04137	Mitophagy - animal	4	63	1.71	1.15e-05	9606.ENSP00000037243, 9606.ENSP00000302564, 9606.ENSP00000358072, 9606.ENSP00000360266
hsa04720	Long-term potentiation	4	64	1.71	1.18e-05	9606.ENSP00000215832, 9606.ENSP00000263025, 9606.ENSP00000272298, 9606.ENSP00000290277
hsa05221	Acute myeloid leukemia	4	66	1.69	1.30e-05	9606.ENSP00000215832, 9606.ENSP00000263025, 9606.ENSP00000279488, 9606.ENSP00000290277
hsa05164	Influenza A	5	165	1.39	1.45e-05	9606.ENSP00000162749, 9606.ENSP00000215832, 9606.ENSP00000263025, 9606.ENSP00000311032, 9606.ENSP00000351273
hsa05140	Leishmaniasis	4	70	1.67	1.54e-05	9606.ENSP00000215832, 9606.ENSP00000216160, 9606.ENSP00000263025, 9606.ENSP00000360266
hsa05214	Glioma	4	72	1.66	1.68e-05	9606.ENSP00000215832, 9606.ENSP00000263025, 9606.ENSP00000272298, 9606.ENSP00000290277
hsa05212	Pancreatic cancer	4	73	1.65	1.73e-05	9606.ENSP00000215832, 9606.ENSP00000263025, 9606.ENSP00000290277, 9606.ENSP00000302564
hsa05203	Viral carcinogenesis	5	182	1.35	2.10e-05	9606.ENSP00000215832, 9606.ENSP00000263025, 9606.ENSP00000311032, 9606.ENSP00000351273, 9606.ENSP00000360266
hsa01521	EGFR tyrosine kinase inhibitor resistance	4	78	1.62	2.12e-05	9606.ENSP00000215832, 9606.ENSP00000263025, 9606.ENSP00000290277, 9606.ENSP00000302564
hsa04012	ErbB signaling pathway	4	83	1.59	2.63e-05	9606.ENSP00000215832, 9606.ENSP00000263025, 9606.ENSP00000290277, 9606.ENSP00000360266
hsa05014	Amyotrophic lateral sclerosis	6	352	1.14	2.63e-05	9606.ENSP00000037243, 9606.ENSP00000162749, 9606.ENSP00000247178, 9606.ENSP00000302564, 9606.ENSP00000311032, 9606.ENSP00000349205
hsa05205	Proteoglycans in cancer	5	196	1.32	2.75e-05	9606.ENSP00000215832, 9606.ENSP00000263025, 9606.ENSP00000290277, 9606.ENSP00000311032, 9606.ENSP00000340944
hsa05235	PD-L1 expression and PD-1 checkpoint pathway in cancer	4	88	1.57	3.09e-05	9606.ENSP00000215832, 9606.ENSP00000263025, 9606.ENSP00000340944, 9606.ENSP00000360266
hsa04912	GnRH signaling pathway	4	89	1.56	3.16e-05	9606.ENSP00000215832, 9606.ENSP00000263025, 9606.ENSP00000272298, 9606.ENSP00000360266
hsa04933	AGE-RAGE signaling pathway in diabetic complications	4	98	1.52	4.48e-05	9606.ENSP00000215832, 9606.ENSP00000263025, 9606.ENSP00000311032, 9606.ENSP00000360266
hsa04014	Ras signaling pathway	5	226	1.26	4.93e-05	9606.ENSP00000215832, 9606.ENSP00000263025, 9606.ENSP00000272298, 9606.ENSP00000302564, 9606.ENSP00000340944
hsa04064	NF-kB signaling pathway	4	101	1.51	4.93e-05	9606.ENSP00000162749, 9606.ENSP00000216160, 9606.ENSP00000302564, 9606.ENSP00000360242
hsa04726	Serotonergic synapse	4	108	1.48	6.13e-05	9606.ENSP00000215832, 9606.ENSP00000263025, 9606.ENSP00000290277, 9606.ENSP00000311032
hsa05135	Yersinia infection	4	125	1.42	0.00011	9606.ENSP00000215832, 9606.ENSP00000216160, 9606.ENSP00000263025, 9606.ENSP00000360266
hsa05168	Herpes simplex virus 1 infection	6	479	1.01	0.00012	9606.ENSP00000162749, 9606.ENSP00000216160, 9606.ENSP00000302564, 9606.ENSP00000311032, 9606.ENSP00000340944, 9606.ENSP00000351273
hsa04270	Vascular smooth muscle contraction	4	133	1.39	0.00013	9606.ENSP00000215832, 9606.ENSP00000263025, 9606.ENSP00000272298, 9606.ENSP00000290277
hsa04910	Insulin signaling pathway	4	133	1.39	0.00013	9606.ENSP00000215832, 9606.ENSP00000263025, 9606.ENSP00000272298, 9606.ENSP00000290277
hsa04915	Estrogen signaling pathway	4	133	1.39	0.00013	9606.ENSP00000215832, 9606.ENSP00000263025, 9606.ENSP00000272298, 9606.ENSP00000360266
hsa05162	Measles	4	138	1.37	0.00014	9606.ENSP00000302564, 9606.ENSP00000311032, 9606.ENSP00000351273, 9606.ENSP00000360266
hsa05034	Alcoholism	4	144	1.35	0.00016	9606.ENSP00000215832, 9606.ENSP00000263025, 9606.ENSP00000272298, 9606.ENSP00000290277
hsa05224	Breast cancer	4	145	1.35	0.00016	9606.ENSP00000215832, 9606.ENSP00000263025, 9606.ENSP00000290277, 9606.ENSP00000360266

(*continued*)

Supplementary Table S2. Continued

Term ID	Term Description	Observed Gene Count	Background Gene Count	Strength	False Discovery Rate	Matching Proteins in Your Network (IDs)
hsa04932	Nonalcoholic fatty liver disease	4	148	1.34	0.00017	9606.ENSP00000162749, 9606.ENSP00000311032, 9606.ENSP00000351273, 9606.ENSP00000360266
hsa04217	Necroptosis	4	149	1.34	0.00018	9606.ENSP00000162749, 9606.ENSP00000216274, 9606.ENSP00000351273, 9606.ENSP00000360242
hsa04921	Oxytocin signaling pathway	4	149	1.34	0.00018	9606.ENSP00000215832, 9606.ENSP00000263025, 9606.ENSP00000272298, 9606.ENSP00000360266
hsa05165	Human papillomavirus infection	5	325	1.1	0.00022	9606.ENSP00000162749, 9606.ENSP00000215832, 9606.ENSP00000263025, 9606.ENSP00000311032, 9606.ENSP00000351273
hsa05225	Hepatocellular carcinoma	4	160	1.31	0.00022	9606.ENSP00000215832, 9606.ENSP00000263025, 9606.ENSP00000290277, 9606.ENSP00000302564
hsa05213	Endometrial cancer	3	57	1.63	0.00026	9606.ENSP00000215832, 9606.ENSP00000263025, 9606.ENSP00000290277
hsa04730	Long-term depression	3	59	1.62	0.00028	9606.ENSP00000215832, 9606.ENSP00000263025, 9606.ENSP00000290277
hsa05120	Epithelial cell signaling in Helicobacter pylori infection	3	67	1.56	0.00040	9606.ENSP00000311032, 9606.ENSP00000340944, 9606.ENSP00000360266
hsa05223	Non-small cell lung cancer	3	68	1.56	0.00041	9606.ENSP00000215832, 9606.ENSP00000263025, 9606.ENSP00000290277
hsa05169	Epstein-Barr virus infection	4	193	1.23	0.00042	9606.ENSP00000216160, 9606.ENSP00000311032, 9606.ENSP00000351273, 9606.ENSP00000360266
hsa04622	RIG-I-like receptor signaling pathway	3	70	1.54	0.00044	9606.ENSP00000351273, 9606.ENSP00000358072, 9606.ENSP00000425107
hsa04510	Focal adhesion	4	198	1.22	0.00045	9606.ENSP00000215832, 9606.ENSP00000263025, 9606.ENSP00000360242, 9606.ENSP00000360266
hsa04115	p53 signaling pathway	3	72	1.53	0.00046	9606.ENSP00000302564, 9606.ENSP00000311032, 9606.ENSP00000351273
hsa05218	Melanoma	3	72	1.53	0.00046	9606.ENSP00000215832, 9606.ENSP00000263025, 9606.ENSP00000290277
hsa04024	cAMP signaling pathway	4	208	1.2	0.00052	9606.ENSP00000215832, 9606.ENSP00000263025, 9606.ENSP00000272298, 9606.ENSP00000360266
hsa04662	B-cell receptor signaling pathway	3	78	1.5	0.00056	9606.ENSP00000215832, 9606.ENSP00000263025, 9606.ENSP00000360266
hsa04658	Th1 and Th2 cell differentiation	3	87	1.45	0.00075	9606.ENSP00000215832, 9606.ENSP00000263025, 9606.ENSP00000360266
hsa04713	Circadian entrainment	3	92	1.42	0.00087	9606.ENSP00000215832, 9606.ENSP00000263025, 9606.ENSP00000272298
hsa05222	Small cell lung cancer	3	92	1.42	0.00087	9606.ENSP00000302564, 9606.ENSP00000311032, 9606.ENSP00000360242
hsa04914	Progesterone-mediated oocyte maturation	3	94	1.42	0.00090	9606.ENSP00000215832, 9606.ENSP00000263025, 9606.ENSP00000290277
hsa04916	Melanogenesis	3	95	1.41	0.00092	9606.ENSP00000215832, 9606.ENSP00000263025, 9606.ENSP00000272298
hsa05215	Prostate cancer	3	96	1.41	0.00094	9606.ENSP00000215832, 9606.ENSP00000263025, 9606.ENSP00000290277
hsa05231	Choline metabolism in cancer	3	96	1.41	0.00094	9606.ENSP00000215832, 9606.ENSP00000263025, 9606.ENSP00000360266
hsa04659	Th17 cell differentiation	3	101	1.38	0.0011	9606.ENSP00000215832, 9606.ENSP00000263025, 9606.ENSP00000360266
hsa04660	TCR signaling pathway	3	101	1.38	0.0011	9606.ENSP00000215832, 9606.ENSP00000263025, 9606.ENSP00000360266
hsa04928	Parathyroid hormone synthesis, secretion and action	3	103	1.38	0.0011	9606.ENSP00000215832, 9606.ENSP00000263025, 9606.ENSP00000290277
hsa04071	Sphingolipid signaling pathway	3	116	1.32	0.0015	9606.ENSP00000162749, 9606.ENSP00000215832, 9606.ENSP00000263025
hsa04114	Oocyte meiosis	3	120	1.31	0.0017	9606.ENSP00000215832, 9606.ENSP00000263025, 9606.ENSP00000272298
hsa05016	Huntington disease	4	298	1.04	0.0017	9606.ENSP00000247178, 9606.ENSP00000311032, 9606.ENSP00000349205, 9606.ENSP00000351273

(*continued*)

Supplementary Table S2. Continued

Term ID	Term Description	Observed Gene Count	Background Gene Count	Strength	False Discovery Rate	Matching Proteins in Your Network (IDs)
hsa04926	Relaxin signaling pathway	3	128	1.28	0.0019	9606.ENSP00000215832, 9606.ENSP00000263025, 9606.ENSP00000360266
hsa05418	Fluid shear stress and atherosclerosis	3	130	1.27	0.0020	9606.ENSP00000162749, 9606.ENSP00000272298, 9606.ENSP00000360266
hsa05226	Gastric cancer	3	144	1.23	0.0027	9606.ENSP00000215832, 9606.ENSP00000263025, 9606.ENSP00000290277
hsa04072	Phospholipase D signaling pathway	3	147	1.22	0.0028	9606.ENSP00000215832, 9606.ENSP00000263025, 9606.ENSP00000340944
hsa04261	Adrenergic signaling in cardiomyocytes	3	147	1.22	0.0028	9606.ENSP00000215832, 9606.ENSP00000263025, 9606.ENSP00000272298
hsa04150	mTOR signaling pathway	3	151	1.21	0.0029	9606.ENSP00000162749, 9606.ENSP00000215832, 9606.ENSP00000263025
hsa04218	Cellular senescence	3	150	1.21	0.0029	9606.ENSP00000215832, 9606.ENSP00000263025, 9606.ENSP00000272298
hsa05216	Thyroid cancer	2	36	1.66	0.0033	9606.ENSP00000215832, 9606.ENSP00000263025
hsa04022	cGMP–PKG signaling pathway	3	162	1.18	0.0034	9606.ENSP00000215832, 9606.ENSP00000263025, 9606.ENSP00000272298
hsa04960	Aldosterone-regulated sodium reabsorption	2	37	1.64	0.0034	9606.ENSP00000215832, 9606.ENSP00000263025
hsa05206	MicroRNAs in cancer	3	160	1.18	0.0034	9606.ENSP00000215832, 9606.ENSP00000263025, 9606.ENSP00000311032
hsa04360	Axon guidance	3	177	1.14	0.0044	9606.ENSP00000215832, 9606.ENSP00000263025, 9606.ENSP00000340944
hsa04930	Type II diabetes mellitus	2	46	1.55	0.0051	9606.ENSP00000215832, 9606.ENSP00000263025
hsa04015	Rap1 signaling pathway	3	202	1.08	0.0062	9606.ENSP00000215832, 9606.ENSP00000263025, 9606.ENSP00000272298
hsa04810	Regulation of actin cytoskeleton	3	209	1.07	0.0068	9606.ENSP00000215832, 9606.ENSP00000263025, 9606.ENSP00000290277
hsa05134	Legionellosis	2	55	1.47	0.0069	9606.ENSP00000311032, 9606.ENSP00000351273
hsa05416	Viral myocarditis	2	55	1.47	0.0069	9606.ENSP00000311032, 9606.ENSP00000351273
hsa04370	VEGF signaling pathway	2	57	1.46	0.0073	9606.ENSP00000215832, 9606.ENSP00000263025
hsa04929	GnRH secretion	2	63	1.41	0.0087	9606.ENSP00000215832, 9606.ENSP00000263025
hsa04664	Fc epsilon RI signaling pathway	2	66	1.39	0.0094	9606.ENSP00000215832, 9606.ENSP00000263025
hsa05012	Parkinson disease	3	240	1.01	0.0094	9606.ENSP00000272298, 9606.ENSP00000302564, 9606.ENSP00000311032
hsa05031	Amphetamine addiction	2	66	1.39	0.0094	9606.ENSP00000272298, 9606.ENSP00000360266
hsa04520	Adherens junction	2	67	1.39	0.0095	9606.ENSP00000215832, 9606.ENSP00000263025
hsa04917	Prolactin signaling pathway	2	69	1.37	0.0099	9606.ENSP00000215832, 9606.ENSP00000263025
hsa04920	Adipocytokine signaling pathway	2	69	1.37	0.0099	9606.ENSP00000162749, 9606.ENSP00000340944
hsa05230	Central carbon metabolism in cancer	2	69	1.37	0.0099	9606.ENSP00000215832, 9606.ENSP00000263025
hsa05020	Prion disease	3	265	0.97	0.0118	9606.ENSP00000215832, 9606.ENSP00000263025, 9606.ENSP00000311032
hsa04540	Gap junction	2	87	1.27	0.0149	9606.ENSP00000215832, 9606.ENSP00000263025
hsa04666	Fc gamma R-mediated phagocytosis	2	90	1.26	0.0158	9606.ENSP00000215832, 9606.ENSP00000263025
hsa04350	TGF-beta signaling pathway	2	91	1.25	0.0160	9606.ENSP00000215832, 9606.ENSP00000263025
hsa04066	HIF-1 signaling pathway	2	106	1.19	0.0211	9606.ENSP00000215832, 9606.ENSP00000263025
hsa04931	Insulin resistance	2	107	1.18	0.0214	9606.ENSP00000162749, 9606.ENSP00000340944

(*continued*)

Supplementary Table S2. Continued

Term ID	Term Description	Observed Gene Count	Background Gene Count	Strength	False Discovery Rate	Matching Proteins in Your Network (IDs)
hsa04725	Cholinergic synapse	2	110	1.17	0.0223	9606.ENSP00000215832, 9606.ENSP00000263025
hsa04724	Glutamatergic synapse	2	111	1.17	0.0225	9606.ENSP00000215832, 9606.ENSP00000263025
hsa04151	PI3K–Akt signaling pathway	3	350	0.84	0.0236	9606.ENSP00000215832, 9606.ENSP00000263025, 9606.ENSP00000302564
hsa04935	Growth hormone synthesis, secretion and action	2	118	1.14	0.0249	9606.ENSP00000215832, 9606.ENSP00000263025
hsa04919	Thyroid hormone signaling pathway	2	119	1.14	0.0251	9606.ENSP00000215832, 9606.ENSP00000263025
hsa04611	Platelet activation	2	122	1.13	0.0261	9606.ENSP00000215832, 9606.ENSP00000263025
hsa05017	Spinocerebellar ataxia	2	135	1.08	0.0313	9606.ENSP00000247178, 9606.ENSP00000349205
hsa04550	Signaling pathways regulating pluripotency of stem cells	2	140	1.07	0.0333	9606.ENSP00000215832, 9606.ENSP00000263025
hsa04723	Retrograde endocannabinoid signaling	2	145	1.05	0.0353	9606.ENSP00000215832, 9606.ENSP00000263025
hsa04934	Cushing syndrome	2	153	1.03	0.0387	9606.ENSP00000215832, 9606.ENSP00000263025
hsa04630	Jak–STAT signaling pathway	2	160	1.01	0.0417	9606.ENSP00000302564, 9606.ENSP00000340944
hsa05202	Transcriptional misregulation in cancer	2	171	0.98	0.0469	9606.ENSP00000279488, 9606.ENSP00000302564

Abbreviations: Akt, protein kinase B; ID, identification; KEGG, Kyoto Encyclopedia of Genes and Genomes; PI3K, phosphoinositide 3-kinase; PKG, protein kinase G; STAT, signal transducer and activator of transcription; Th1, T helper 1; Th17, T helper 17; Th2, T helper 2.

Matching Proteins in Your Network (Labels)
GABARAPL2, MAPK1, TAB1, RIPK3, MAPK3, BCL2L1, CASP8, ATG5, XIAP, JUN, ATG12
GABARAPL2, MAPK1, ATG14, MAPK3, ATG3, BCL2L1, PIK3R4, ATG5, DAPK1, ATG12
GABARAPL2, TNFRSF1A, MAPK1, TAB1, ATG14, MAPK3, BCL2L1, PIK3R4, ATG5, JUN, ATG12
GABARAPL2, TNFRSF1A, MAPK1, ATG14, MAPK3, CALM2, ATG3, CASP3, CASP8, JUN
TNFRSF1A, MAPK1, TAB1, MAPK3, BCL2L1, CASP3, CASP8, XIAP
TNFRSF1A, MAPK1, TAB1, RIPK3, MAPK3, CASP3, CASP8, JUN
TNFRSF1A, MAPK1, TAB1, MAPK3, CALM2, BCL2L1, CASP3, CASP8, JUN
TNFRSF1A, MAPK1, MAPK3, BCL2L1, CASP3, CASP8, XIAP, JUN
TNFRSF1A, MAPK1, TAB1, MAPK3, CASP3, PTPN11, CASP8, JUN
TNFRSF1A, MAPK1, TAB1, RIPK3, MAPK3, CASP3, CASP8, JUN
TNFRSF1A, MAPK1, ATG14, MAPK3, CALM2, ARAF, CASP3, PIK3R4, CASP8
MAPK1, MAPK3, CALM2, ARAF, BCL2L1, CASP3, CASP8, XIAP, JUN, DAPK1
MAPK1, MAPK3, BCL2L1, CASP3, CASP8, XIAP
GABARAPL2, ATG3, PIK3R4, ATG5, ATG12
TNFRSF1A, BCL2L1, CASP3, CASP8, XIAP
MAPK1, TAB1, MAPK3, ARAF, CASP3, CASP8, JUN
TNFRSF1A, MAPK1, TAB1, MAPK3, DUSP6, ARAF, CASP3, JUN
MAPK1, MAPK3, CALM2, PTPN11, CASP8, JUN
MAPK1, MAPK3, ARAF, PTPN11, JUN
TNFRSF1A, MAPK1, MAPK3, ARAF, CASP3, CASP8
MAPK1, MAPK3, CALM2, CASP3, JUN
MAPK1, MAPK3, ARAF, BCL2L1, PTPN11
TNFRSF1A, MAPK1, MAPK3, CALM2, CASP3, CASP8
MAPK1, MAPK3, ARAF, CASP3, JUN
MAPK1, MAPK3, CASP3, CASP8, JUN
MAPK1, BIK, MAPK3, ARAF, JUN
TNFRSF1A, MAPK1, MAPK3, CASP8, JUN
MAPK1, TAB1, MAPK3, CASP8, JUN
TNFRSF1A, MAPK1, MAPK3, BCL2L1, XIAP, JUN
TNFRSF1A, MAPK1, MAPK3, CALM2, CASP3, CASP8
MAPK1, MAPK3, ARAF, DAPK1
MAPK1, MAPK3, CALM2, PTPN11, JUN
MAPK1, MAPK3, ARAF, CASP3, PTPN11
TNFRSF1A, MAPK1, TAB1, MAPK3, JUN
GABARAPL2, MAPK1, MAPK3, ARAF, ATG12
GABARAPL2, MAPK1, MAPK3, CALM2, PIK3R4
GABARAPL2, BCL2L1, ATG5, JUN
MAPK1, MAPK3, CALM2, ARAF
MAPK1, MAPK3, DUSP6, ARAF
TNFRSF1A, MAPK1, MAPK3, CASP3, CASP8
MAPK1, TAB1, MAPK3, JUN
MAPK1, MAPK3, CALM2, ARAF
MAPK1, MAPK3, ARAF, BCL2L1
MAPK1, MAPK3, CASP3, CASP8, JUN
MAPK1, MAPK3, ARAF, BCL2L1
MAPK1, MAPK3, ARAF, JUN
GABARAPL2, TNFRSF1A, ATG14, BCL2L1, CASP3, PIK3R4
MAPK1, MAPK3, ARAF, CASP3, PTPN11
MAPK1, MAPK3, PTPN11, JUN
MAPK1, MAPK3, CALM2, JUN
MAPK1, MAPK3, CASP3, JUN
MAPK1, MAPK3, CALM2, BCL2L1, PTPN11
TNFRSF1A, TAB1, BCL2L1, XIAP
MAPK1, MAPK3, ARAF, CASP3
MAPK1, TAB1, MAPK3, JUN

(*continued*)

Continued

Matching Proteins in Your Network (Labels)
TNFRSF1A, TAB1, BCL2L1, CASP3, PTPN11, CASP8
MAPK1, MAPK3, CALM2, ARAF
MAPK1, MAPK3, CALM2, ARAF
MAPK1, MAPK3, CALM2, JUN
BCL2L1, CASP3, CASP8, JUN
MAPK1, MAPK3, CALM2, ARAF
MAPK1, MAPK3, ARAF, JUN
TNFRSF1A, CASP3, CASP8, JUN
TNFRSF1A, RIPK3, CASP8, XIAP
MAPK1, MAPK3, CALM2, JUN
TNFRSF1A, MAPK1, MAPK3, CASP3, CASP8
MAPK1, MAPK3, ARAF, BCL2L1
MAPK1, MAPK3, ARAF
MAPK1, MAPK3, ARAF
CASP3, PTPN11, JUN
MAPK1, MAPK3, ARAF
TAB1, CASP3, CASP8, JUN
CASP8, ATG5, ATG12
MAPK1, MAPK3, XIAP, JUN
BCL2L1, CASP3, CASP8
MAPK1, MAPK3, ARAF
MAPK1, MAPK3, CALM2, JUN
MAPK1, MAPK3, JUN
MAPK1, MAPK3, JUN
MAPK1, MAPK3, CALM2
BCL2L1, CASP3, XIAP
MAPK1, MAPK3, ARAF
MAPK1, MAPK3, CALM2
MAPK1, MAPK3, ARAF
MAPK1, MAPK3, JUN
MAPK1, MAPK3, JUN
MAPK1, MAPK3, JUN
MAPK1, MAPK3, ARAF
TNFRSF1A, MAPK1, MAPK3
MAPK1, MAPK3, CALM2
ATG14, CASP3, PIK3R4, CASP8
MAPK1, MAPK3, JUN
TNFRSF1A, CALM2, JUN
MAPK1, MAPK3, ARAF
MAPK1, MAPK3, PTPN11
MAPK1, MAPK3, CALM2
TNFRSF1A, MAPK1, MAPK3
MAPK1, MAPK3, CALM2
MAPK1, MAPK3
MAPK1, MAPK3, CALM2
MAPK1, MAPK3
MAPK1, MAPK3, CASP3
MAPK1, MAPK3, PTPN11
MAPK1, MAPK3
MAPK1, MAPK3, CALM2
MAPK1, MAPK3, ARAF
CASP3, CASP8
CASP3, CASP8
MAPK1, MAPK3
MAPK1, MAPK3
MAPK1, MAPK3
CALM2, BCL2L1, CASP3
CALM2, JUN

(*continued*)

Continued

Matching Proteins in Your Network (Labels)
MAPK1, MAPK3
MAPK1, MAPK3
TNFRSF1A, PTPN11
MAPK1, MAPK3
MAPK1, MAPK3, CASP3
MAPK1, MAPK3
MAPK1, MAPK3
MAPK1, MAPK3
MAPK1, MAPK3
TNFRSF1A, PTPN11
MAPK1, MAPK3
MAPK1, MAPK3
MAPK1, MAPK3, BCL2L1
MAPK1, MAPK3
MAPK1, MAPK3
MAPK1, MAPK3
ATG14, PIK3R4
MAPK1, MAPK3
MAPK1, MAPK3
MAPK1, MAPK3
BCL2L1, PTPN11
DUSP6, BCL2L1

Abbreviations: ID, identification; KEGG, Kyoto Encyclopedia of Genes and Genomes; Th17, T helper 17.